Analysis of mammography screening schedules under varying resource constraints for planning breast cancer control programs in low- and middle- income countries: a mathematical study

*Shifali Bansal[1], BS, *Vijeta Deshpande[1], MS, Xinmeng Zhao[1], BS, Jeremy A. Lauer[2], PhD, Filip Meheus[3], PhD, André Ilbawi[2], MD, Chaitra Gopalappa[1], PhD

*equal contribution

[1]University of Massachusetts- Amherst, Massachusetts, United States

[2]World Health Organization, Geneva, Switzerland

[3]International Agency for Research on Cancer, Lyon, France

Word Count: 5946

Corresponding author: Chaitra Gopalappa, chaitrag@umass.edu

Funding: *The study was partly supported by a grant from the World Health Organization. The funding agreement ensured the authors' independence in designing the study, interpreting the data, writing, and publishing the report. The following authors are employed by the sponsor: Jeremy A. Lauer and André Ilbawi.*

Work conducted at: University of Massachusetts Amherst, Massachusetts, USA; World Health Organization, Geneva, Switzerland; and International Agency for Research on Cancer, Lyon, France.

Conference presentation: Work presented at INFORMS Annual Meeting, November 2018, Phoenix, AZ

INFORMS Healthcare, July 2019, Cambridge, MA

INFORMS Annual Meeting, October 2019, Seattle, WA

Disclaimer: Where authors are identified as personnel of the International Agency for Research on Cancer / World Health Organization, the authors alone are responsible for the views expressed in this article and they do not necessarily represent the decisions, policy or views of the International Agency for Research on Cancer / World Health Organization.

Abstract

Background

Low-and-middle-income countries (LMICs) have higher mortality-to-incidence ratio for breast cancer compared to high-income countries (HICs) because of late-stage diagnosis. Mammography screening is recommended for early diagnosis, however, the infrastructure capacity in LMICs are far below that needed for adopting current screening guidelines. Current mammography screening guidelines are extrapolations from HICs as limited data had restricted model development specific to LMICs, and thus, economic analysis of screening schedules specific to infrastructure capacities are unavailable.

Methods

We applied a new Markov-process method for developing cancer progression models and a Markov decision process model to identify optimal screening schedules under varying number of lifetime screenings per person, a proxy for infrastructure capacity. We modeled Peru, a middle-income country as case study, and the United States (US), a HIC for validation.

Results

Implementing 2, 3, 5, 10, and 15 lifetime screens would require about 55, 85, 135, 280, and 405 mammography machines, respectively, and save 31, 44, 62, 95, and 112 life-years per 1000 women, respectively. Current guidelines recommend 15 lifetime screens but Peru only has 55 mammography machines nationally. With current capacity, the best strategy is 2 lifetime screenings at age 50 and 56. As infrastructure is scaled-up to accommodate 3, 5, and 10 lifetime screens, screening between age 46 and 57, 44 and 61, and 41 and 64, respectively, would have the best impact. Our results for the US are consistent with other models and current guidelines.

Limitations

The scope of our model is limited to analysis of national-level guidelines, we did not model heterogeneity across the country.

Conclusions

Country-specific optimal screening schedules under varying infrastructure capacities can systematically guide development of cancer control programs and planning of health investments.

Introduction

Breast cancer is the most common and frequent cancer among women globally. According to the World Health Organization (WHO), (1) it is estimated that 627,000 women died from breast cancer in 2018, which accounts for approximately 15% of all cancer deaths among women. Approximately 70% of deaths from cancers occur in low- and middle- income countries (LMICs) which can partly be associated with late stage diagnosis when survival is low, about 70-90% of breast cancer cases in LMICs get diagnosed in late stages compared to 40% in the United States (US). (2), (3), (4) It is estimated that 1.7 million new cases of breast cancer will present in the developing world in 2020, and the huge discrepancy in survival chances will continue with most of the breast cancer deaths (70%) occurring in the developing world. (5) More generally, cancer is the second leading cause of premature deaths globally, accounting for about 17% of deaths, and 60% of all premature deaths are from non-communicable diseases (NCDs). In addition to the disease burden, the economic burden of NCDs such as breast cancer is also considerably high. It is estimated that the economic losses in LMICs from NCDs are equivalent to approximately 4% of current annual national economic outputs. (6)

To address this growing disease and economic burden, the 70th World Health Assembly adopted the updated Appendix 3 of the Global NCD Action Plan for 2013-2020, which is a list of the 'Best Buys' interventions proposed by the World Health Organization (WHO) to reduce premature mortality from NCDs by 25% by 2025. (7), (8)

Individual countries are further conducting NCD 'investment cases', which includes quantitative economic analysis of current and potentially implementable health interventions. (9) The objective of a national investment case is to identify prioritized and coherent investments that are tailored to the country's needs and resource availabilities through evaluations of both potential returns on investment and cost of inaction. (9), (10), (11)

In this paper, we present a modeling approach to identify optimal mammography screening schedules for early detection of breast cancer. Early detection will enable early treatment, which is key for reducing premature mortalities. Peru was used as a case study. Current model-based analysis informing mammography guidelines in LMICs are based on extrapolations of impacts from high-income countries (HICs). (12) This is because of data limitations in LMICs that create barriers to parameterizing a natural disease progression model specific to the population. (13), (14) In this work, we first parameterized a natural disease progression model using a two-step Markov process methodology (15) developed specific to the data-settings in LMICs. Further, to base the analysis not only on disease burden but also on the resource availabilities in Peru, instead of comparative analysis of a few preselected scenarios as commonly done, we used Markov decision processes to identify best screening schedules under varying resource constraints.

Methodology

Natural onset and progression of breast cancer

We assumed that breast cancer initiates as carcinoma in-situ (CIS), i.e., women can transition from healthy to CIS. In the absence of diagnosis, the disease naturally progresses through preclinical invasive carcinoma local, regional, and distant stages (Figure 1). From any of these preclinical stages, women can transition to clinical stages through diagnosis based on symptoms or through screening. Upon clinical diagnosis, women remain in the stage at diagnosis and face a certain rate of death based on stage-specific survival rates.

Two-step Markov process methodology for parametrization of cancer model specific to LMICs

Parameterization of a cancer natural history model consists of estimation of three sets of parameters that vary by age: a) onset rates- the rates of transitioning from healthy to CIS; b) progression rates- the rates of transitioning between preclinical disease stages in the absence of diagnosis, and c) diagnostic rates- the current rates of diagnosis in the absence of intervention. Though there are multiple mathematical models presented in the literature for parameterization of natural history models, most are applied to HICs and are

based on the use of longitudinal data from cancer registries (16), (17), (18), (19) or population-based screening studies. (20), (21) The pre- and post- screening data provide references for the estimation process. Data that are usually available for most LMICs are only the nationally representative annual rates of cancer incidence and mortality, i.e., the numbers of newly diagnosed cases of cancers and deaths per 1000 women, estimated through the Global Cancer Observatory. (2), (22) There are usually no data on how people are diagnosed, which could vary according to population-specific parameters, such as population's awareness and knowledge in recognizing symptoms and access to health care, in addition to disease-specific parameters such as occurrence of symptoms. Therefore, in this study, we used a new two-step Markov process methodology developed specifically for parameterization of cancer progression models in LMICs where longitudinal cancer registry databases are not available. (15) This method, under the assumption that progression rates are disease-specific and do not vary by population, uses pre-estimated progression rates from the literature (Appendix A), and estimates population-specific onset rates and diagnostic rates by fitting Markov process models to data on invasive cancer incidence and stage at diagnosis from Peru (Table S3 in Appendix A). The mathematical structure of the model generates onset rates to be representative of CIS cases that may or may not progress to invasive carcinoma within the lifetime of the individual, although it does not incorporate cases of CIS that may regress. The model generates diagnostic rates to be representative of the overall rates of diagnosis in the population, inclusive of the inverse of stage-dependent time for development of symptoms and time-delays in seeking care, and thus inclusive of population's awareness to symptoms and access to care. Based on estimates in the literature (23), we assumed that progression rates are a logistic function of age, with progression being more aggressive at younger ages.

Technical details of the theory and proofs of the parameterization methodology are presented in (15) and its application for the analysis of the 'Best Buy' interventions, for breast cancer, cervical cancer, and colorectal cancer for updating the Appendix 3 of the NCD Global Action Plan (8), (7) are presented in (24).

Markov decision process (MDP) model for identifying optimal mammography screening schedules

Typically, in the public health literature, optimal screening schedules are identified through comparative evaluations between a few pre-selected scenarios on certain metrics such as life-years saved or mortality reduction. In the case of mammography screening for informing population-level guidelines, specific screening schedules are evaluated, e.g., biennial screening for age group 40 to 69 years or annual screening for age group 50 to 69 years. (25) In this paper, we instead identify optimal screening schedules from among all possible combinations of age groups and screening intervals, by formulating the problem as a Markov decision process (MDP) and solving it using dynamic programming (DP).

The MDP is a sequential decision-making model. Specifically, for any given screening schedule, it can evaluate the weighted average lifetime costs and benefits, weighted according to the probabilities of cancer onset by age and its progression under the influence of the screening schedule. It uses the Markov process model discussed in the previous section to determine the probabilities. DP is an optimization method used with MDP. Instead of exhaustively evaluating all possible choices for screening schedule, which can be a very large number, DP uses mathematical concepts to identify the optimal screening schedules through evaluation of only a few sampled choices. (26)

We define an optimal screening schedule as one that gives the best trade-offs between costs and benefits. Costs include screening costs, follow-up diagnosis costs for true-positives and false positives, and treatment costs. Benefits include quality-adjusted life-years (QALYs) saved compared to no screening. To convert benefits into the same metrics as costs, they are multiplied with a monetary value-per-QALY lived. Value-per-QALY is a measure for the economic value added from health investments. (27) For any specific assumption for the value-per-QALY, an MDP model can identify the screening schedule, including the optimal number of lifetime screens, that give the best trade-offs in costs and benefits. We can expect that as the value-per-QALY lived increases, the optimal schedule will have higher number of lifetime screens. Researchers have suggested multiple assumptions for the value-per-QALY lived, several related to the GDP per capita of the country, and thus, could change over time and vary by country. (27) Therefore, instead of

assuming a constant value, we evaluate different assumptions for value-per-QALY lived to generate different optimal number of lifetime screens.

MDP models are extensively used in engineering applications, and some studies have applied it to mammography screening decisions, most for individual-level clinical decision-making, specifically, whether to screen or not based on a woman's medical condition and care history and some studies have applied it to population-level screening. (28), (29), (30) In this work, we use MDP for population-level analysis of screening strategies to inform national screening guidelines. We present the mathematical formulation in Appendix B.

Scenarios and Impact measures

Identification of optimal scenarios using MDP model: For any given value-per-QALY, the MDP model outputs all ages at which women should be screened, and thus, the number of lifetime screenings, age for screening initiation, age for screening termination, and the time intervals between screenings can be estimated.

Estimation of impact metrics by Markov process simulation: For each optimal strategy, by simulating the Markov process model over a 100 year period, we calculated the number of life-years (LY) saved per 1000 women, the number of false positives (FP) per 1000 women, costs per 1000 women, and cost per LY saved as per the equations summarized in Table 1. We did not discount benefits or costs.

Estimation of resource (mammography machines) needs: For each optimal scenario, we calculated the number of mammography machines needed per year as the number of screens per year divided by capacity of each mammography machine. We calculated the number of screens per year by adding the number of people in Peru in 2017 in the ages corresponding to the screening schedules. We assume an annual capacity of 5800 tests per mammography machine based on current utilization in some HICs. (31), (32)

Generation of efficient frontier: By plotting life-years saved versus number of lifetime screens and life-years saved versus costs, we generate "efficient frontier" curves to identify non-dominated scenarios. A scenario is non-dominated if it has the highest life-years saved among all scenarios with similar costs, and thus will lie on the efficient frontier.

Comparison of optimal screening schedules with current recommendations: Recommendations for mammography screening vary by issuing entities. For the Americas, the WHO strongly recommends biennial screening for age-group 50 to 69 years (10 lifetime screens), and conditionally recommends screening at other age groups. (33) National guidelines in Peru recommend biennial screening for age-group 40 to 69 (15 lifetime screens), (34) but the WHO recommends against screening persons below age 49 in low-resource settings even with strong health systems. As current recommendations are equivalent of 10 or 15 lifetime screens in our method, we highlight these scenarios for comparing model results with current recommendations.

Base case and sensitivity analyses input assumptions

For Peru, as basecase, we assumed the use of film mammography for breast cancer screening, as the more advanced digital mammography used in high-income countries (HICs) are typically unavailable in LMICs. (33) For basecase analyses, we used the latest estimates for sensitivity and specificity of film mammography. We also used average values for stage progression rates from the literature. To understand the sensitivity of these inputs on results for optimal screening schedules, we conducted the following sensitivity analyses:

a) Sensitivity to limited availability of latest film mammography technology and expertise – Estimates from the breast cancer surveillance consortium (BCSC) suggests that mammography sensitivity and specificity have been increasing over time, representing the advancements in diagnostic tools. Therefore, we used mammography specificity and sensitivity from the 1995-1999 era to test the impact of the unavailability of the most recent technology and human expertise. Data assumptions are presented in Appendix D1.

b) Sensitivity to dwell times (inverse of progression rates) by stage - We tested a range of values, using estimates from different models in the literature to set the lower and upper bounds. This sensitivity analysis represents the uncertainty in natural rates of stage progression. Data assumptions are represented in Appendix D2.

c) Uncertainty analysis on CIS pathways (5 CIS cases): Recent studies, under the context of over-diagnosis of cancers, have highlighted the uncertainty around pathways of CIS stage and mammography sensitivity for diagnosis at this stage, and their corresponding impact on the progression rate estimates for CIS. Therefore, as uncertainty analysis, we evaluated 5 CIS cases, each using different combinations of CIS progression rate, proportion of invasive cancers initiating directly in local stage, and mammography sensitivity in CIS stage. Data assumptions under each of the 5 CIS cases are presented in Appendix D3.

Model Validation

For validating our model, we applied it to the United States (US) population for comparison with results from the CISNET (The Breast Cancer Working Group of the Cancer Intervention and Surveillance Modeling Network (25)) study, a study that used 6 independent models to inform current screening guidelines globally. (12) Data for model parameterization were extracted from the CISNET studies and are presented in the Appendix (Tables S3 and S7). We conducted the following two sets of validation.

a. Validation of impact estimates: Unlike the MDP method that identifies optimal schedules, the method used in the CISNET study is comparative analysis of a few pre-selected screening schedules. (25) We evaluated these pre-selected schedules using our model and extracted impact measures. To keep consistent with results presented in the CISNET study, we did not discount these impact measures.

Results: Our estimation of benefits and harms, life-years (LY) saved per 1000 women and false positives per 1000 women, respectively, under different screening schedules compare well with CISNET model results (Figure S5 in Appendix C). (25) Cost estimations from the 6 CISNET models range from

USD 2·9 to 5·62 million per 1000 women for the no-screening scenario, and our model estimates a cost of USD 3·7 per 1000 women for the same. Cost estimations from the 6 CISNET models ranged from 5·02 to 6·15 million per 1000 women for screening schedule of biennial 50 to 74 (B50-74) and for this scenario our model estimates a cost of 6·2 million per 1000 women. (35) Further, the scenarios identified as non-dominated in our MDP model are also classified as efficient or borderline in the CISNET study (25) (Figure S6 in Appendix C). The CISNET study classified a scenario as 'efficient' if it was non-dominated in at least 5 models and as 'borderline' if it was dominated in 2 to 4 models.

b. Validation of the MDP method of selecting optimal schedules: To demonstrate the advantage of using the MDP model to identify an 'optimal' screening schedule, instead of using pre-selected schedules as commonly done, we applied the MDP model to the US population. We identified optimal screening schedules for up to 20 lifetime screens. We combined the optimal schedules identified by the MDP model and the CISNET pre-selected schedules to generate an efficient frontier by plotting life-years saved per 1000 women against number of lifetime screens, and life-years saved per 1000 women against costs per 1000 women (Figure S7 in Appendix C).

Results: There are two notable results from this comparison. First, all the screening schedules identified as optimal by the MDP model are either on or close to the efficient frontier curve, demonstrating that the MDP model can identify the most efficient strategies (Figure S7 in Appendix C). Second, the MDP model helps identify the minimum number of lifetime screens, for the US it suggests a minimum of 10. We verify the validity of this result by using our model to specifically evaluate and compare cost per life-year saved under 10 lifetime screens with that of lower number of lifetime screens. The schedule with 10 lifetime screens had a lower cost per life-year saved than schedules with 5 (B60-69) and 8 (B55-69) lifetime screens, the latter two are preselected schedules evaluated in the CISNET study (Table S9 in Appendix C).

Results

The model predictions for the optimal screening schedule under alternative choices in lifetime number of screens, and corresponding benefits, harms, and costs, are presented in Table 2. All values are undiscounted. The table also presents the number of mammography machines needed nationally, to implement the strategy in Peru. While the model suggests a minimum of 10 lifetime screens for the US (Validation section), for Peru, the model suggests a minimum of 1 screen. This implies that, for the US, the costs of screening are offset by the costs saved from early stage diagnosis of cancers, late stage diagnosis have much higher treatment costs (Table S7 in Appendix B). As unit costs for screening and treatment are higher for the US than Peru, to test the sensitivity of these cost differences, we reevaluated Peru using US costs. Under this, the minimum number of lifetime screens for Peru increased to 5, suggesting that the differences in minimum lifetime screens are due to the differences in both costs and disease burden, disease burden being higher in the US.

Figure 2 plots optimal age intervals to screen under different choices of lifetime screens. For Peru, under 15 lifetime screens, the model estimated that the optimal age-interval to screen is 40 to 67 years, and estimated that this scenario would result in 112 life-years saved per 1000 women and 1302 false positives per 1000 women. Under 10 lifetime screens, the model estimated that the optimal age-interval to screen is 41 to 64 years, and estimated that this scenario would result in about 95 life-years saved and 939 false positives per 1000 women (Figure 3). Current screening guidelines recommend biennial screening between ages 40 to 69 (B40-69) (15 lifetime screens) and biennial screening between ages 50 to 69 (B50-69) (10 lifetime screens). Specifically evaluating these current guidelines using our model generated about 109 life-years saved and 1267 false positives per 1000 women under B40-69, and about 66 life-years saved and 814 false positives per 1000 women under B50-69 (data not plotted). Therefore, while our model results agree with the current recommendations under 15 lifetime screens, under 10 lifetime screens the model suggests screening should start at a younger age.

For comparison, we also used the MDP model to estimate the optimal age-intervals to screen for the US (Figure 2). Under 15 lifetime screens, the model estimated that the optimal age-interval to screen is

41 to 69 years, and under 10 lifetime screens the optimal age-interval to screen is 47 to 68 years. These results are close to the current WHO recommendations of biennial 40 to 69 years or biennial 50 to 69 years, respectively. The model estimates for the corresponding number of life-years saved per 1000 women were 169 and 132, respectively, and corresponding number of false positives per 1000 women were 1264 and 841, respectively (Figure 3).

The model estimates for false positives per 1000 women were equivalent for the US and Peru, which is as expected because of similar assumptions for screening specificity. The number of life years saved per 1000 women were much higher in the US compared to Peru, (Figure 3) which is as expected because of higher incidence rates for breast cancer in the US (Table S3 in Appendix A). The model estimated that, while the number of life-years saved would have diminishing returns with increase in the number of lifetime screens, the number of false positives per 1000 women would increase linearly with increase in the number of lifetime screens.

For Peru, the model estimated optimal age-group for screening was around 50 to 55 years for up to 2 lifetime screens, 45 to 62 years for up to 6 lifetime screens, 40 to 65 years up to 11 lifetime screens, and 40 to 68 years for higher lifetime screens. The lowest age, even going up to 18 lifetime screens was 40. As the number of lifetime screens increased, the upper bound of screening interval increased. The screening frequency under a given scenario of lifetime screens was not uniform (Figure 4).

For Peru, the model estimated general trend was more frequent screening between ages 44 and 54 years, e.g., under 10 lifetime screens, the optimal schedule was biennial screening for age group 44 to 54, triennial for age groups 41 to 44 and 54 to 60, and the last screen was at age 64 after a 4-year gap (Figure 4).

For implementing these schedules in Peru, the number of mammography machines needed would range from 29 under 1 lifetime screen to 488 under 18 lifetime screens (Table 2). Currently, there is a total of about 55 mammography machines available nationally in public hospitals in Peru. (31), (32)

For Peru, the model estimated lifetime costs for breast cancer was USD 53,000 per 1000 women for no screening and ranged from USD 136,000 per 1000 women for 1 lifetime screen to about USD 1·1 million per 1000 women for 18 lifetime screens (Table 2). Cost per life-year saved ranged from USD 4,300 for scenario with 1 lifetime screen to USD 8,400 for scenario with 18 lifetime screens (Table 2). These results are generally in the range of results from other models for Peru. (36) All benefits and costs are undiscounted.

The efficient frontier generated by plotting undiscounted life-years saved v. undiscounted costs per 1000 women is presented in Figure 5 for Peru. The graph plots both optimal schedules from our MDP model, under alternative choices of lifetime screens, and pre-selected schedules from CISNET. Results indicate that most of the scenarios in the CISNET study that are efficient for the US are not efficient for Peru, the exception being biennial 40-69 years which corresponds to 15 lifetime screens.

Results for sensitivity analyses are presented in Appendix D. Lowering the sensitivity and specificity of film mammography, compared to the basecase, had minimal impact on the age-interval for screening. However, under any given number of lifetime screens, it reduced life-years saved and increased false-positives, and thus, increased the cost per life-year saved from USD 4,400 to 6,500 under 1 lifetime screen and USD 7,500 to 13,800 under 15 lifetime screens. Varying stage-specific dwell times shifted the age-intervals for screening by a few years, shifting towards the older or younger ages when the dwell times decreased or increased, respectively. The corresponding outcomes on false positives and total costs saw minimal changes, but the life-years saved increased or decreased when dwell times decreased or increased, respectively. Thus, the costs per life-year saved under 1 lifetime screen were between $4,100 and $5,200 for the lower and upper values of dwell times, respectively, as compared to $4,400 in basecase. The costs per life-year saved under 5 lifetime screens were between $4,300 and $5,900 for the lower and upper values of dwell times, respectively, as compared to $5,000 in the basecase. All benefits and costs are undiscounted.

Uncertainty around assumptions related to the CIS stage had the most impact on screening schedules. Under CIS case 1, where the CIS dwell time was kept the same but its sensitivity to mammography screening was set at about half of that in basecase, the starting age to screen shifted towards older ages, while the end age stayed the same resulting in more uniform time-intervals between screens. Up until 4 lifetime screens the starting age to screen was age 50, while in the basecase, this varied between 50 under 1 lifetime screen to 45 under 4 lifetime screens. Up until 9 lifetime screens the starting age to screen was 45, while in the basecase, this varied between 45 under 4 lifetime screens to 40 under 9 lifetime screens. Results under CIS cases 2, 3, and 4 were alike and, like in Case 1, suggest to initiate screening at an older age than that in basecase, but unlike Case 1, suggest to also stop screening at an older age than that in basecase. Cases 2 and 3 assumed a very low average dwell time (3 and 5 months) compared to the basecase (5.22 years). Case 4 assumed an average dwell time of 2 years and, additionally, assumed 18.9% of cancer cases initiated directly at local stage as opposed to 0% in basecase, and a mammography sensitivity for CIS stage at about half of that in basecase. Under CIS cases 2, 3, and 4, the youngest age for screening initiation was about 50 years up until 6 lifetime screens, and 45 years up until 10 lifetime screens. CIS uncertainty analysis Case 5 assumed an average dwell time of 15 years for CIS, the proportion of cancers initiating directly at local stage as 18.9%, and a mammography sensitivity for CIS stage at about half of that in basecase. Under CIS case 5, the starting age to screen is similar to the basecase but the end age to screen shifted towards a younger age. Screening was contained between ages 40 to 60 years, suggesting that cancers developing after age 60 are less likely to progress to invasive cancers within the lifetime of individuals because of the lengthy average dwell time. Similar shifts in screening intervals were also observed for the US under CIS Cases 1 to 5. This uncertainty in CIS pathways under Cases 1 to 5, while had minimal impact on false positives and total costs, had a relatively significant impact on life-years saved and thus, costs per life-year saved. While the cost per life-year saved for the basecase varied between USD 4,400 and USD 7,500 for lifetime screens between 1 and 15, respectively, it varied between USD 6,800 and 10,800 in CIS Case 1, between USD 11,300 and 14,400 in CIS Case 2, between USD 10,900 and 14,000 in

CIS Case 3, between USD 9,300 and 12,800 in CIS Case 4, and between USD 6,900 and 11,500 in CIS Case 5. All benefits and costs are undiscounted.

Discussion and Conclusions

This paper presents a new methodology for parameterization of cancer natural onset and progression for data-limited settings such as Peru, and application of a MDP model for estimating optimal screening schedules under different assumptions for value-per-QALY lived to impose constraints on the number of lifetime screens. Though current literatures present multiple Markov processes-based parameterization methodologies and MDP models for identifying screening options, most are applied to or derived from application to populations in HICs. As noted by other researchers in systematic reviews of economic evidence for informing breast cancer strategies for LMICs, the quality of studies specific to LMICs are poor due to lack of data availability. (13), (37), (38) Countries thus resort to extrapolating strategies or impacts of strategies from HICs, which is challenging as multiple factors, including health systems and infrastructure availability, vary by country. The parameterization methodology used in this paper was specific to data availabilities in LMIC settings.

Currently, for high resource settings, WHO strongly recommends biennial screening between ages 50 to 69, and conditional biennial screening between ages 40 to 49 and 70 to 75 years. For low resource settings, it recommends conditional biennial screening between ages 50 to 69 and recommends against screening between ages 40 to 49 and 70 to 75. (33) The latter because of higher number of false positives (positive testing of a woman with no cancer) and over diagnosis (treatment of cancers that may not progress) observed for these ages, requiring resources for careful monitoring and evaluation that maybe unavailable in low-resource settings. (33)

The results from the model for the US are generally in agreement with above guidelines. In contrast, under the same number of lifetime screens, the optimal age intervals to screen in Peru are shifted towards younger ages. Possible reasons are differences in disease risk and other cause mortality. For

instance, compared to the US, in Peru, incidence rates are lower, pre-screening incidence risk by age increases at a slower rate, and average life-expectancy is 5 years shorter (Table S3 in Appendix A).

Results for optimal screening schedules under alternative constraints on the number of lifetime screens, presented here, are especially of interest if resource availabilities and/or population's compliance to screening limits the implementation of the recommended 10 or 15 lifetime screens. For instance, Peru currently has about 55 mammography machines nationally in public hospitals. (31), (32) Our results indicate that, assuming 100% compliance, this would be sufficient for implementing 2 lifetime screens and, under this constraint, screening at ages 50 and 56 would provide best outcomes. Results under alternative number of lifetime screens are helpful for systematically planning health investments. For instance, our results indicate that implementing 5 lifetime screens will require about 136 machines nationally, i.e., addition of infrastructure and human resources for another 81 machines. Further, during investment planning, decision-makers should additionally consider geographical accessibility to testing centers and population density in allocation of mammography testing centers. Among the 55 machines currently available in Peru, 4 (~7.3%) are in urban areas of the northern region, (31), (32) about 9.35 % of women older than 50 years live in this region. (31)

For the US, the model suggests a minimum of 10 lifetime screens as optimal, the average undiscounted cost per life-year saved for 10 lifetime screens were lower than scenarios with lower number of lifetime screens. For Peru, the model suggests that even 1 lifetime screen has benefits that outweigh costs. However, the paper presents optimal screening schedules under 1 to 18 number of lifetime screens and the selection of the choice in number of lifetime screens should be based on careful consideration of associated benefits, harms, and costs. As the number of lifetime screens increased, the number of life-years saved increased, however, at a slower rate than the number of false positives. These higher rates of false positives have critical implications for health system resource allocation. False positive findings result in billions of dollars of added expenditure in the US. (39), (40), (41) In this work, our assumption for follow-up costs for a false positive were about 13% of a true positive, however, we did not model and consider the

costs of over diagnosis. Increased number of total tests resulting from over diagnosis can over burden the system which is especially a problem in countries like Peru where current capacities are already insufficient. (31)

Sensitivity analysis on the effectiveness of mammography screening suggests that even if the availability of advanced technology and expertise are limited, the screening intervals do not change. Uncertainty analysis on CIS pathways, Cases 1 to 5, had the most impact on the age intervals to screen and on the costs per life-years saved estimates. Interpretation of these results should be done alongside the mathematical interpretation of the inputs in our model. First, our model estimates onset rates to specifically fit to incidence rates by age and stage, and for Peru, this represents invasive cancer incidence because about 97% of incident cases were diagnosed in stages local, regional, or distant, and only 3% in CIS. Second, we do not model CIS cases that regress and only model progressive CIS cases, however, progressive cases may or may not progress to invasive cancer within the lifetime of the individual, the proportion progressing dependent on the assumptions for the average CIS dwell time. Third, as the model assigns a QALY of 1 for all preclinical stages, less than 1 for all clinical stages, and 0 for deaths (Table S7 in Appendix B), screening of cases that do not progress to invasive cancer within the lifetime of an individual will contribute negative benefits while also adding to costs. Finally, in identifying an optimal screening scenario, the MDP model considers the trade-offs between total costs (screening and treatment) and benefits (QALYs saved) and thus incorporates the dis-benefits of treating cases that might have never progressed within the lifetime.

Under this mathematical structure, the basecase and CIS Case 1 will both have similar progressions to invasive cancer. The differences in screening intervals between the two suggests to delay screening if the technological ability to detect CIS is low. In CIS cases 2 and 3, because of the short dwell times, the chance of getting diagnosed in CIS were very low resulting in much lower life-years saved as mortality rates are higher once they progress to invasive cancer. Case 4 creates a similar setting as Cases 2 and 3 because of a combination of short dwell time, low mammography sensitivity, and a fraction of cases starting directly as invasive cancer. In Case 5, screening after age 60 had little impact because of the lengthy CIS

average dwell time, suggesting that most cases originating after age 60 would not progress to invasive cancer within the individual's lifetime. These results, under the mathematical structure of our model, suggests that an understanding of the CIS pathways for progressive cancer cases (inclusive of those that do not progressive within individual's lifetime) and screening effectiveness in detecting CIS cases are to be considered in determining the age interval to screen. Under all 5 CIS cases, the differences in screening intervals between the US and Peru persisted, suggesting that screening guidelines should be evaluated specific to each population.

The model is subject to limitations. We only considered heterogeneity by age for incidence and did not consider any other causal factors such as diet, alcohol and tobacco consumption, or genetics. For women who were diagnosed, we did not explicitly model recurrence of disease, we only applied an average stage-and-age-specific rate of survival. We assumed that all women diagnosed with the disease receive treatment and, upon disease onset, its natural progression in preclinical stages only vary by age and stage. We did not model heterogeneity in cancer subtypes between different populations, or the family history of cancer. We did not model over-diagnosis of cancers, we only modeled false positives incorporated as costs in the MDP model. We did not model CIS cases that can regress and are screen detectable due to the unavailability of data for estimating rates specific to the country, thus our model did not consider the costs and disability associated with unnecessary treatment of these cases. Uncertainty analysis suggests that CIS pathways and mammography sensitivity are key factors in informing guidelines and these factors should be studied more specifically to the country, assessing the availability of human expertise and technological infrastructure for accurate diagnosis of progressive cancers. This work is suitable for informing national-level mammography screening guidelines specific to a country and for planning infrastructure scale-ups, implementation of cancer control programs should be studied separately to consider the broader context of cancer control interventions. In construction of the model for the US for validation with CISNET results, we did not consider the full set of data used in the CISNET models such as incidence and mortality that varied as a function of time, but only used the point estimates publicly available through their publications.

Despite these limitations, we believe the paper makes several significant contributions. Our analysis suggests that though current infrastructure is insufficient for implementing current mammography guidelines, efficient use of current infrastructure can significantly reduce mortalities. The methodologies presented here can help develop efficient mammography intervention programs that are more tailored to the country, including its disease risk, resource availabilities, and preferences. It can help inform an 'investment case', a national plan for systematically scaling-up infrastructure and strengthening health systems. Finally, the methodology presented here is a promising option for evaluating interventions in combination for multiple types of cancers, for analysis related to mortality reduction goals pledged by countries under the Sustainable Development Goals. (8) As the number of interventions increases, it is tedious and infeasible to exhaustively evaluate pre-select interventions. This paper demonstrates that the MDP method of using mathematical concepts to identify an optimal scenario is an effective alternative.

References

1. World Health Organization. Breast cancer. [Online]. [cited 2019 May 12. Available from: https://www.who.int/cancer/prevention/diagnosis-screening/breast-cancer/en/.

2. Ferlay J, Soerjomataram I, Ervik M, Dikshit R, Eser S, Mathers C, et al. GLOBOCAN 2012: estimated cancer incidence, mortality and prevalence worldwide in 2012. Int J Cancer. 2012; 136:E359-86.

3. Harford J, Otero I, Anderson B, Cazap E, Gradishar W, Gralow J, et al. Problem solving for breast health care delivery in low and middle resource countries (LMCs): consensus statement from the Breast HealtGlobal Initiative. The Breast. 2011 Apr 1; 20: p. S20-S29.

4. Kamangar F, Dores G, Anderson W. Patterns of cancer incidence, mortality, and prevalence across five continents: defining priorities to reduce cancer disparities in different geographic regions of the world. Journal of clinical oncology. 2006 May 10; 24(14): p. 2137-50.

5. Torre LA, Bray F, Siegel RL, Ferlay J, Lortet-Tieulent J, Jemal A. Global cancer statistics, 2012. CA: a cancer journal for clinicians. 2015; 65(2): p. 87-108.

6. Bloom DE, Chisholm D, Jane-Llopis E, Prettner K, Stein A, Feigl A. From Burden to "Best Buys": Reducing the Economic Impact of Non-Communicable Disease in Low- and Middle-Income Countries. ; 2011.

7. World Health organization. CANCER INTERVENTIONS TECHNICAL BRIEFING. [Online].: WHO; 2017 [cited 2019 March 18. Available from: https://www.who.int/ncds/governance/Cancers-FINAL-18May.pdf?ua=1.

8. World Health Organization. Tackling NCDs: 'best buys' and other recommended interventions for the prevention and control of noncommunicable diseases. [Online].: WHO; 2017 [cited 2019 March 18. Available from: https://apps.who.int/iris/handle/10665/259232.

9. World Health Organization. Noncommunicable diseases and their risk factors. [Online].; 2018 [cited 2018 June 5. Available from: http://www.who.int/ncds/un-task-force/events/economist-training-2018/en/.

10. World Health Organization , United Nations Development Programme. Launch of NCD Investment Case in Mongolia. [Online].; 2018 [cited 2018 June 5. Available from: https://www.who.int/ncds/un-task-force/invest-ncds-mongolia/en/.

11. World Health Organization. Global Health Observatory data repository. [Online].; 2016 [cited 2019 March 18. Available from: http://apps.who.int/gho/data/node.main.A914?lang=en.

12. International Agency for Research on Cancer. Breast cancer screening Volume 15. Lyon Cedex 08, France:; 2016.

13. Zelle SG, Baltussen RM. Economic analyses of breast cancer control in low-and middle-income countries: a systematic review. Systematic reviews. 2013; 2(1): p. 20.

14. Anderson BO, Ilbawi AM, El Saghir NS. Breast cancer in low and middle income countries (LMICs): a shifting tide in global health. The breast journal. 2015; 21(1): p. 111-118.

15. Gopalappa C, Guo J, Meckoni P, Munkhbat B, Pretorius C, Lauer J, et al. A Two-Step Markov Processes Approach for Parameterization of Cancer State-Transition Models for Low-and Middle-Income Countries. Medical Decision Making. 2018; 38(4): p. 520-530.

16. Mandelblatt J, Schechter C, Lawrence W, Yi B, Cullen J. Chapter 8: The spectrum population model of the impact of screening and treatment on US breast cancer trends from 1975 to 2000: Principles and practice of the model methods. JNCI Monographs. 2006 Oct 1; 36: p. 47-55.

17. Tan SY, Oortmarssen GJv, Koning HJd, Boer R, Habbema JDF. The MISCAN-Fadia Continuous Tumor Growth Model for Breast Cancer. 2006; 36.

18. Tan K, Simonella L, Wee H, Roellin A, Lim Y, Lim W, et al. Quantifying the natural history of breast cancer. British journal of cancer. 2013 Oct; 109(8): p. 2035.

19. Fryback D, Stout N, Rosenberg M, Trentham-Dietz A, Kuruchittham V, Remington P. Chapter 7: The Wisconsin breast cancer epidemiology simulation model. JNCI Monographs. 2006 Oct 1; 36: p. 37-47.

20. Duffy S, Day N, Tabár L, Chen H, Smith T. Markov models of breast tumor progression: some age-specific results. JNCI Monographs. 1997 Jan 1; 22: p. 93-7.

21. Tabar , Vitak , Chen , Prevost , Duffy. Update of the Swedish Two-County Trial of breast cancer screening: histologic grade-specific and age-specific results. Swiss surgery. 1999 Oct 1; 5(5): p. 199-204.

22. Torre L, Bray F, Siegel R, Ferlay J, Lortet-Tieulent J, Jemal A. Global cancer statistics, 2012. CA Cancer J Clin. 2015 March 01; 65(2): p. 87-108.

23. Zelle SG, Baltussen R, Otten JD, Heijnsdijk EA, van Schoor G, Broeders MJ. Predicting the stage shift as a result of breast cancer screening in low-and middle-income countries: a proof of concept. Journal of medical screening,. 2015; 22(1): p. 8-19.

24. Ralaidovy AH, Gopalappa C, Ilbawi A, Pretorius C, Lauer JA. Cost-effective interventions for breast cancer, cervical cancer, and colorectal cancer: new results from WHO-CHOICE. Cost Effectiveness and Resource Allocation. 2018; 16(1): p. 38.

25. Mandelblatt JS, Cronin KA, Bailey S, Berry DA, Koning HJD, Draisma G, et al. Effects of Mammography Screening Under Different Screening Schedules Model Estimates of Potential Benefits and Harms. Annals of internal medicine. 2009 November 14; 151(10): p. 738-747.

26. Zhang J, Mason JE, Denton BT, Pierskalla WP. Applications of operations research to the prevention, detection, and treatment of disease. Wiley Encyclopedia of Operations Research and Management. Wiley. 2011.

27. Jamison DT, Summers LH, Alleyne G, Arrow KJ, Berkley S, Binagwaho A, et al. Global health 2035: a world converging within a generation. The Lancet. 2013; 382(9908): p. 1898-1955.

28. Ayer T, Alagoz O, Stout NK. OR Forum—A POMDP approach to personalize mammography screening decisions. Operations Research. 2012; 60(5): p. 1019-1034.

29. Kong Q, Mondschein S. Optimal Guidelines for Screening Mammography Based on Individual Risk Factors. [Online].; 2015 [cited 2019 March 18. Available from: https://ssrn.com/abstract=2646902.

30. Maillart LM, Ivy JS, Ransom S, Diehl K. Assessing dynamic breast cancer screening policies. Operations Research. 2008; 56(6): p. 1411-1427.

31. Bain C, Constant TH, Contreras I, Vega AMB, Jeronimo J, Tsu V. Model for Early Detection of Breast Cancer in Low-Resource Areas: The Experience in Peru. Journal of global oncology. 2018; 4: p. 1-7.

32. Autier P, Ouakrim DA. Determinants of the number of mammography units in 31 countries with significant mammography screening. British journal of cancer. 2008; 7(99): p. 1185.

33. World Health Organization. WHO position paper on mammography screening. [Online].: WHO Library Cataloguing-in-Publication Data; 2014 [cited 2019 March 18. Available from: http://www.who.int/iris/handle/10665/137339.

34. PAHO, WHO Cancer Country profiles. paho.org. [Online].; 2013 [cited 2018 June 8. Available from: http://www.paho.org/hq/index.php?option=com_topics&view=rdmore&cid=5642&Itemid=40735&lang=en.

35. Stout NK, Lee SJ, Schechter CB, Kerlikowske K, Alagoz O, Berry D, et al. Benefits, harms, and costs for breast cancer screening after US implementation of digital mammography. JNCI: Journal of the National Cancer Institute. 2014; 106(6).

36. Zelle SG, Vidaurre T, Abugattas JE, Manrique JE, Sarria G, Jeronimo J, et al. Cost-effectiveness analysis of breast cancer control interventions in Peru. PLoS One. 2013; 8(12): p. e82575.

37. Birnbaum JK, Duggan C, Anderson BO, Etzioni R. Early detection and treatment strategies for breast cancer in low-income and upper middle-income countries: a modelling study. The Lancet Global Health. 2018; 6(8): p. e885-e893.

38. Islam RM, Billah B, Hossain N, Oldroyd J. Barriers to Cervical Cancer and Breast Cancer Screening Uptake in Low-Income and Middle-Income Countries: A Systematic Review. Asian Pacific journal of cancer prevention: APJCP. 2017; 18(7): p. 1751.

39. Vlahiotis A, Griffin B, Stavros AT, Margolis J. Analysis of utilization patterns and associated costs of the breast imaging and diagnostic procedures after screening mammography. ClinicoEconomics and outcomes research: CEOR. 2018; 10: p. 157.

40. Chubak J, Boudreau DM, Fishman PA, Elmore JG. Cost of breast-related care in the year following false positive screening mammograms. Medical care. 2010; 48(9): p. 815.

41. Mandrik O, Zielonke N, Meheus F, Severens JL, Guha N, Herrero Acosta R, et al. Systematic reviews as a "lens of evidence": determinants of benefits and harms of breast cancer screening. International journal of cancer. 2019.

42. Forbes. Forbes. [Online]. [cited 2018 March 10. Available from: https://www.forbes.com/places/peru/.

43. International Agency for Research on Cancer, World Health Organization. Global cancer observatory. [Online].; 2012 [cited 2018 February 12. Available from: http://globocan.iarc.fr/Pages/age-specific_table_sel.aspx.

Life years saved per 1000 women in a screening scenario compared to no screening = $\frac{10^3(L_{screening}-L_{basecase})}{L_{basecase}/t_{avg}}$

False positives per 1000 women in no-screening scenario = $\frac{10^3 N_{FP}}{L_{basecase}/t_{avg}}$

Costs per 1000 women = $\frac{10^3(c_{screen}N_{screens}+c_{FP}N_{FP}+c_{TP}N_{TP}+c_I N_I+c_T N_T)}{L_{basecase}/t_{avg}}$

Cost per LY saved = $\frac{Cost\ per\ 1000\ women\ in\ screening\ scenario - Cost\ per\ 1000\ women\ in\ no\ screening}{Life\ years\ saved\ per\ 1000\ women}$

Notation	Description	
$L_{screening}$	Life years lived in the screening scenario (optimal screening) over a 100-year period (While the age-specific mortality rates were applied, the maximum life expectancy was set to 100 years. Therefore, we used a 100-year period to ensure that everyone undergoes the required number of lifetime screens.)	
$L_{basecase}$	Life years lived in the base-case (no screening) over a 100-year period	
t_{avg}	Average life expectancy in Peru	
$\frac{L_{basecase}}{t_{avg}}$	An approximation for the average number of women in the simulation	
c_{screen}	Unit cost of mammography screening	2.54 USD for Peru (24)
c_{FP}	Cost per woman for follow-up diagnostic tests for a false positive case	72.18 USD for Peru (24)
c_{TP}	Cost per woman for follow-up diagnostic tests for a true positive case	551.36 USD for Peru (24)
c_I	Initial treatment cost per woman	Stage / Initial, $ (Peru) (24) / Terminal, $(Peru) In situ 218.01 590 localized 218.01 590 Regional 464.58 787 Distant 684.84 1053 Note: Cost assumptions for the US model are presented in Appendix B Table S7
c_T	Terminal treatment cost per woman, which was applied at the final 12 months of life for women who die of breast cancer. The ratio of terminal to initial costs in the US were used in estimating terminal costs for Peru	
$N_{screens}$	Total number of women who were screened over a 100-year period	
N_{FP}	Total number of false positives over a 100-year period	
N_{TP}	Total number of true positives over a 100-year period	
N_I	Total number of women diagnosed with breast cancer over a 100-year period	

Table 1: Summary of impact metrics estimations and cost assumptions

142x195mm (144 x 144 DPI)

Number of lifetime screenings	Age interval for screening	Number of mammography units needed per year*	False positives per 1000 women	Life-years saved per 1000 women **	QALYs saved per 1000 women **	Total cost per 1000 women (USD)**	Cost per life-year saved (USD)**	Cost per QALY saved (USD) **
0	NA	reference	NA	reference	reference	52,644	reference	reference
1	51-51	29	129	19	22	135,788	4,376	3,825
2	50-56	54	220	31	37	192,122	4,499	3,805
3	46-57	83	315	44	51	252,467	4,541	3,940
4	45-60	109	395	54	62	303,885	4,653	4,056
5	44-61	136	489	62	72	363,927	5,021	4,334
6	44-62	163	579	70	80	421,727	5,273	4,593
7	41-62	197	676	78	89	484,359	5,535	4,877
8	42-63	219	766	84	95	542,360	5,830	5,158
9	42-64	243	842	88	101	591,269	6,121	5,342
10	41-64	278	939	95	107	654,089	6,331	5,609
11	42-65	307	978	99	112	680,196	6,339	5,627
12	41-66	324	1055	101	115	730,554	6,712	5,896
13	40-66	353	1132	105	119	780,415	6,931	6,099
14	41-67	373	1213	107	122	832,693	7,290	6,412
15	40-67	406	1302	112	129	890,442	7,480	6,640
16	40-67	435	1389	114	129	946,532	7,841	6,925
17	40-67	466	1477	117	132	1,003,876	8,130	7,207
18	40-68	488	1551	119	134	1,051,642	8,395	7,440

*Calculated as number of screens per year divided by capacity of each mammography machine; Number of screens per year was calculated by adding the number of people in Peru in 2017 in the ages corresponding to the screening schedules; Assuming capacity of each mammography machine as 5800 tests per year;
** All benefits, harms, and costs are undiscounted

Table 2: Summary of benefits, harms, and costs under alternative screening schedules for Peru.

171x195mm (144 x 144 DPI)

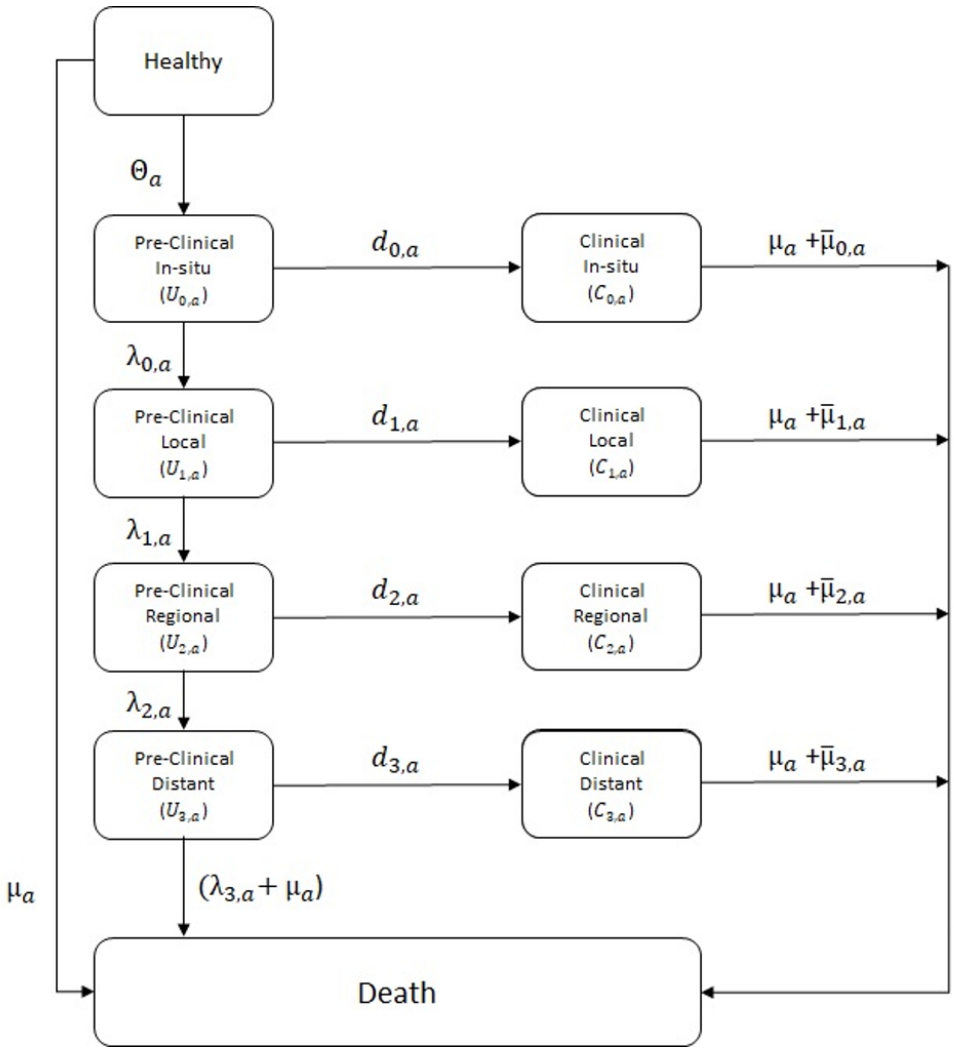

Figure 1: Flow diagram of breast cancer onset and stage progression

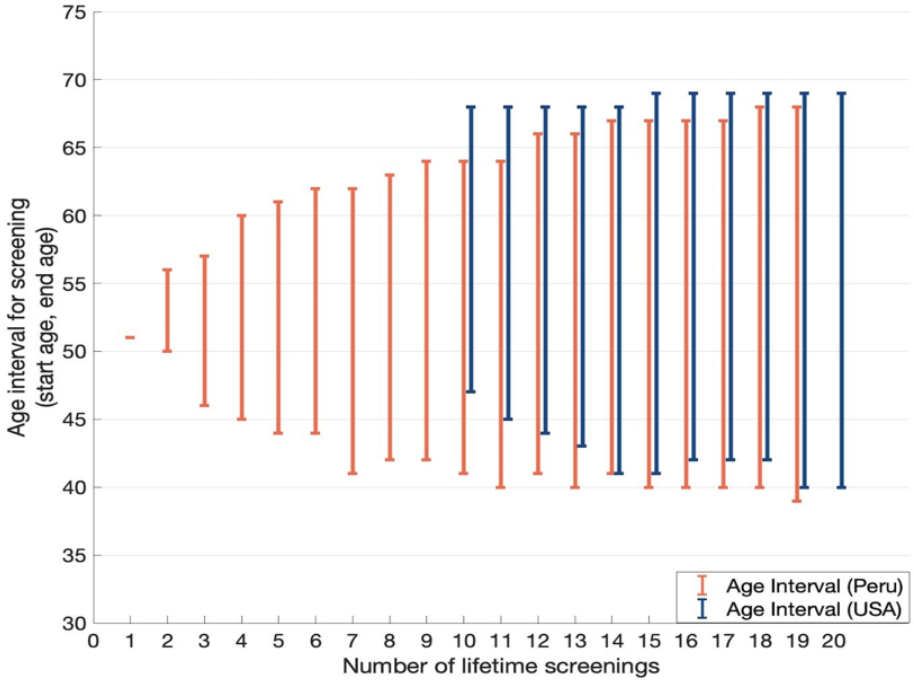

Figure 2: Comparing optimal age-intervals to screen under different choices of lifetime screens

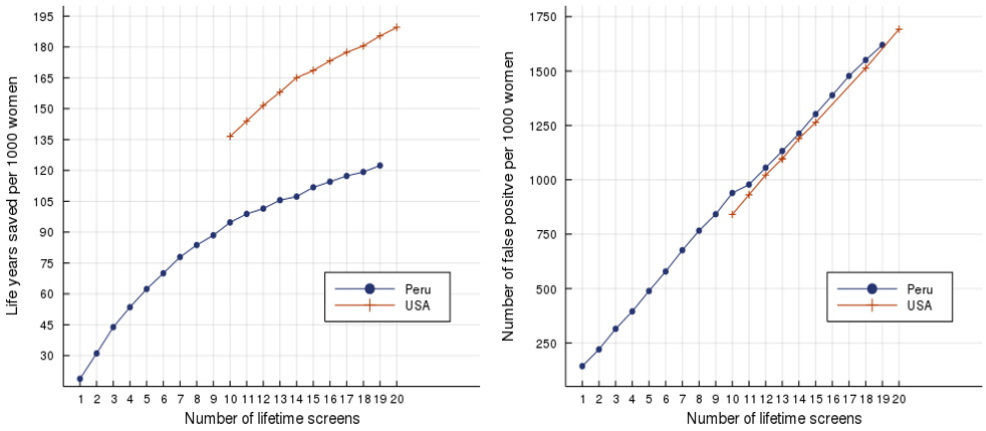

Figure 3: Comparison of life years saved and false positives (FP) under different choices of lifetime screens.

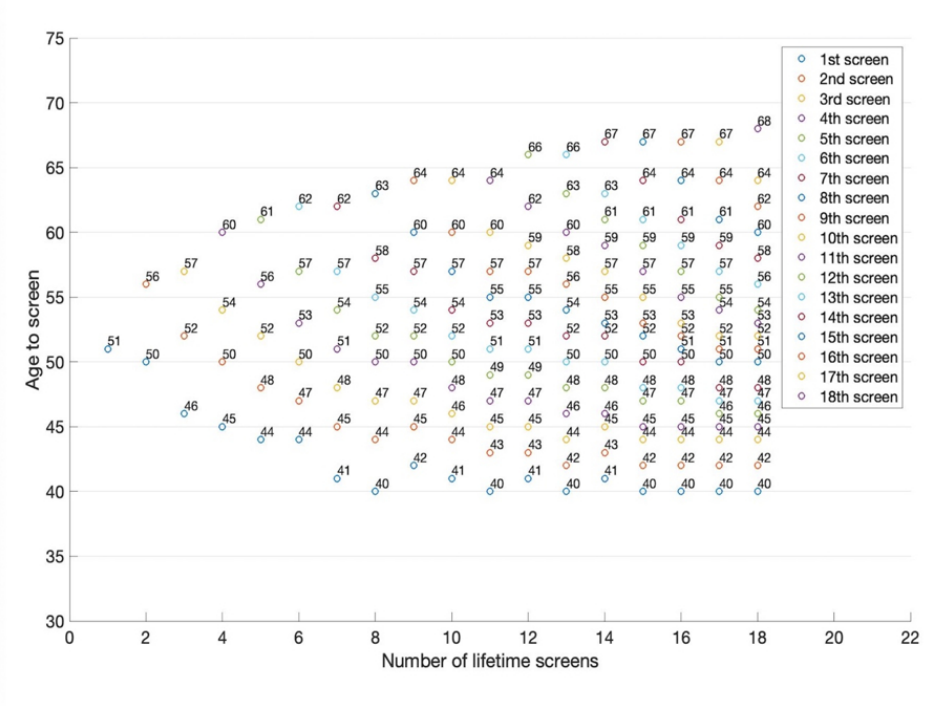

Figure 4: Optimal screening schedule for Peru under different choices of lifetime screens.

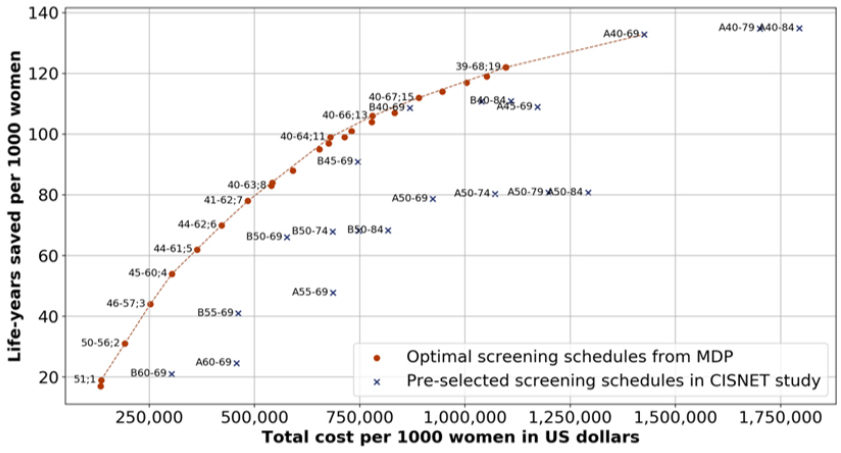

Figure 5: Efficient frontier generated by plotting both pre-selected scenarios in CISNET study and optimal schedules generated by the MDP model for Peru. Legend for data labels: Age interval to screen; Number of lifetime screens. Benefits and costs are undiscounted.

Appendix:

Analysis of mammography screening schedules under varying resource constraints for planning breast cancer control programs in low- and middle- income countries: a mathematical study

Shifali Bansal[1], BS, Vijeta Deshpande[1], MS, Xinmeng Zhao[1], BS, Jeremy A. Lauer[2], PhD, Filip Meheus[3], PhD, André Ilbawi[2], MD, Chaitra Gopalappa[1], PhD

Table of Contents

A. Two-step Markov process (TSMP) methodology for parametrization of the natural onset and progression of cancer

Parameterization of a cancer natural history model consists of estimation of three sets of parameters that vary by age: a) onset rates- the rates of transitioning from healthy to carcinoma in-situ (CIS); b) progression rates- the rates of transitioning between preclinical disease stages in the absence of diagnosis, and c) diagnostic rates- the current rates of diagnosis in the absence of intervention. Though there are multiple mathematical models presented in the literature for parameterization of natural history models, most are applied to HICs and are based on the use of longitudinal data from cancer registries (1), (2), (3), (4) or population-based screening studies. (5), (6) The pre- and post- screening data provide references for the estimation process. Data that are usually available for most LMICs are only the nationally representative annual rates of cancer incidence and mortality, i.e., the numbers of newly diagnosed cases of cancers and deaths per 1000 women, estimated through the Global Cancer Observatory. (7), (8) There are usually no data on how people are diagnosed, which could vary according to population-specific parameters, such as population's awareness and knowledge in recognizing symptoms and access to health care, in addition to disease-specific parameters such as occurrence of symptoms. Therefore, in this study, we used a new two-step Markov process methodology developed specifically for parameterization of cancer progression models in LMICs where longitudinal cancer registry databases are not available. (9)

The TSMP method uses as inputs, country-specific incidence estimates by age, which are publicly available through Global Cancer Observatory, and country-specific stage at diagnosis distributions, which were obtained from studies in the literature. Among the three sets of parameters needed for the model (discussed above), we assumed that the second sets of rates, progression rates, are disease-specific and do not vary by country, and used estimates from models applied to high-income countries that were presented in the literature (see Table S3). We then estimated onset rates and diagnostic rates specific to Peru using the TSMP method. Technical details of the theory and proofs of the TSMP are presented in (9) and its application for the cost-effectiveness analysis of the 'Best Buy' interventions, for breast cancer, cervical cancer, and colorectal cancer for updating the Appendix 3 of the NCD Global Action Plan (10) (11) are presented in (12). In these previous work, the model in (9) was applied to sub-Saharan Africa and Southeast Asia regions using data from 2008 to 2012, when there was not much screening in these regions. However, in the case of Peru, certain populations underwent screening prior to 2012. Therefore, we modified the model in (9) to consider this difference, which we discuss here. For completeness, we first present the earlier version of the model formulation before discussing the modifications specific to Peru.

A.1. Overview of the two-step Markov process method for parametrization of natural history model specific to LMICs

The TSMP divides the estimation of population-specific onset rates of disease and diagnostic rates into two steps, each defined by a Markov process model but with different state spaces. In the first step, we define the disease onset and progression as a discrete-time Markov process $\boldsymbol{X} = \{X_t; t \geq 0, \Omega, \mathbb{P}\}$ with a collapsed state space $\Omega = \{[H_a], [U_a], [D_a]\}$ representing age a and health states H_a =healthy, U_a= undiagnosed, and D_a= diagnosed, without differentiating between disease stages; and $\mathbb{P}$ is the transition probability matrix. We assume that $\mathbb{P}$ is heterogeneous by age, i.e., the probabilities for disease onset, diagnosis, and stage progression were modeled as a function of age. Therefore, the size of the state space is 300, 3 health states time 100 ages. We estimate age-specific onset rates using an iterative analytical model derived using the Markov chain.

In the second step, we estimated diagnostic rates in each stage of cancer, i.e., transition rates from preclinical to clinical states ($d_{i,a}$), by using a simulation-based optimization of the Markov process $\boldsymbol{Y} = \{Y_t; t \geq 0, Z, \mathbb{Q}\}$, with state space $Z = \{[H_a], [U_{i,a}], [D_{i,a}]\}$, which is an expansion of the state space in equation (1) to include stage $i \in \{0 = CIS, 1 = Local, 2 = Regional, and\ 3 = Distant\}$ and age a; and rate matrix $\mathbb{Q}$, which corresponds to the flow diagram in Figure S1.

We discuss each of these steps below.

A.1.1. Estimation of disease onset rates

We use a two-step Markov process for estimation of disease onset rates and diagnostic rates. In this first step, for estimation of the onset rates, we define disease onset and progression as a discrete-time Markov process,

$$\boldsymbol{X} = \{X_t; t \geq 0, \Omega, \mathbb{P}\} \quad (1)$$

with a collapsed state space $\Omega = \{[H_a],[U_a],[D_a]\}$ representing age a and health states H_a =healthy, U_a= Undiagnosed, and D_a= diagnosed, (see Figure S1 for a flow diagram, and Table S1 for a list of notations), without differentiating between disease stages; and $\mathbb{P}$ is the transition probability matrix. Then, using steady state Markov properties we can write

$$\pi_k = \sum_{j \epsilon \Omega,} \pi_j P_{jk} \;; 0 \leq \pi_k \leq 1; \sum_{k \epsilon \Omega} \pi_k = 1 \quad (2)$$

where, P_{jk} are the probabilities of transitioning from state j to state k, i.e., elements of the matrix $\mathbb{P}$, and π_k are the elements of the steady-state distribution vector $\boldsymbol{\pi}$. Our prime element of interest in this Markov process is $P_{H_a U_a}$, the risk or probability of developing the disease in age a, i.e., an element of $\mathbb{P}$ representing the probability of transitioning from H_a to U_a. Using the standard definition of risk to rate conversion that assumes that the underlying distributions governing transition probabilities are exponential, the rate of disease onset in age group a can be written as $\theta_a = -\ln(1 - P_{H_a U_a})$. Based on the above structure of the Markov process we derived an analytical expression for estimation of $P_{H_a U_a}$ as

$$P_{H_a U_a} = \frac{I_{D_a} c_a - \sum_{k=0}^{a-1} \left(\pi_{H_k} P_{H_k U_k} \left[\sum_i s_i \left(1 - e^{-(a-k)\lambda_i}\right) - \sum_i s_i \left(1 - e^{-(a-1-k)\lambda_i}\right) \right] \left(\prod_{j=k:a+1} e^{-\mu_j} \right) \right)}{A_a \left[\sum_i s_i \left(1 - e^{-\lambda_i}\right) \right] \left(e^{-\mu_a}\right) - I_{D_a} c_a} \quad (3)$$

and developed an iterative process for estimation of $P_{H_a U_a}$ starting with the lowest age. We present the notations and the iterative process for estimating of $P_{H_a U_a}$and eventually θ_a in Tables S1 and S2, respectively. The details of the derivation are presented elsewhere. (9)

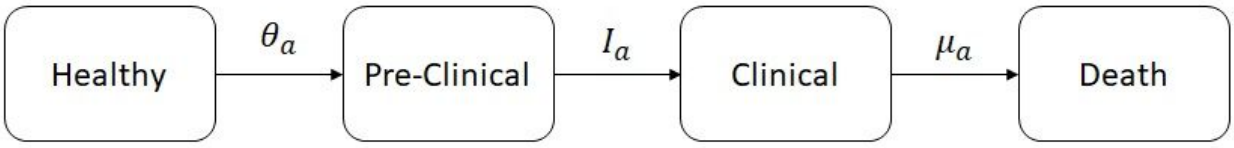

Figure S1: Flow diagram for the collapsed state space in the Markov process used for parameterization of disease progression

Table S1: Summary of notations for estimation of onset rate using algorithm in Table S2

Notation	Description
Model 1: $\boldsymbol{X} = \{X_t; t \geq 0,\ \Omega, \mathbb{P}, \boldsymbol{\pi}\}$	$\boldsymbol{X}$ is a Markov process with state space Ω, its underlying discrete time Markov chain given by the one-step transition probability matrix $\mathbb{P}$ and steady-state distribution vector $\boldsymbol{\pi}$.
$[H_a]$,$[U_a]$,$[D_a]$	Age-vectors representing states of healthy, pre-clinical disease (i.e., undiagnosed cancer state), and clinical disease (i.e., diagnosed cancer state), respectively, for age a
π_j	Element of vector $\boldsymbol{\pi}$ representing steady-state probability for state j
P_{jk}	Element of the matrix $\mathbb{P}$ representing one-step probability of transitioning from state j to k
$P_{H_aU_a} = 1 - e^{-\theta_a}$	$P_{H_aU_a}$ is the risk of developing disease at age a, and is defined as the one-step probability of transitioning from healthy to preclinical disease (H_a *to* U_a); θ_a is the rate of disease onset per person-year among persons in age a (used in Model 2)
T	T is a random variable denoting the time taken to transition to clinical disease state from the time of disease onset (sojourn time); $T \sim hyperexponential(\lambda_1, s_1, \ldots, \lambda_4, s_4)$, s_i is the probability that T will take the form of the exponential distribution with rate λ_i
S	S is a random variable denoting time of natural survival past the age at disease onset (i.e., the person does not die from any other disease during this time) ; $S \sim exponential(\mu_k)$
I_{D_a}	Cancer incidence, defined as the number of new cases of cancer diagnoses in age a each year divided by the number of people in age a
c_a	The proportion of the total population in age a
A_a	Among persons in age group a, the proportion in healthy state or pre-clinical disease states
$p_{i,a}$	Rate of progression from disease stage i to $i+1$ (also used in Model 2)
μ_a	Disease-free mortality rate at age a
Model 2: $\boldsymbol{Y} = \{Y_t; t \geq 0, \mathbb{Z}, \mathbb{Q}, \boldsymbol{\rho}\}$	$\boldsymbol{Y}$ is a continuous time Markov process with state space $\mathbb{Z}$, generator matrix $\mathbb{Q}$, and steady state distribution vector $\boldsymbol{\rho}$.
$[H_a]$,$[U_{i,a}]$,$[D_{i,a}]$	Age-vector representing states of healthy, pre-clinical disease (i.e., undiagnosed cancer state), and clinical disease (i.e., diagnosed cancer state), respectively, at age a and cancer stage i
$\theta_a = -\ln(1 - P_{H_aU_a})$	Rate of disease onset in age a; (see Model 1 for $P_{H_aU_a}$)
$d_{i,a}$	Diagnostic rates, defined as the rates of transitioning from pre-clinical stage i to clinical-stage i per person-year for persons in age a
$p_{i,a}$	Rate of progression from disease stage i to $i+1$ (also used in Model 1)
μ_a	Disease-free mortality rate at age a
$\overline{\mu}_{i,a}$	Mortality rates when not on treatment and at disease stage i and age a
$\overline{\overline{\mu}}_{i,a}$	Mortality rates on treatment and at disease stage i and age a
I_a	Cancer incidence by age a
s_i	Proportion diagnosed in stage i in screening-naïve population

Table S2: Overview of the algorithm for computing age-specific onset rate of cancer

Initialize $\pi_{H_0} = A_0$; $\pi_{U_0} = 0$; and $P_{H_0U_0} = 0$; Set $a = 1$, the youngest age-group of cancer onset (we assumed age 15 for breast cancer).

Step 1: Calculate in-situ onset rate

$$P_{H_aU_a} = \frac{I_{D_a}c_a - \sum_{k=0}^{a-1}\left(\pi_{H_k}P_{H_kU_k}\left[\sum_i s_i\left(1-e^{-(a-k)\lambda_i}\right) - \sum_i s_i\left(1-e^{-(a-1-k)\lambda_i}\right)\right]\left(\prod_{j=k:a+1} e^{-\mu_j}\right)\right)}{A_a\left[\sum_i s_i\left(1-e^{-\lambda_i}\right)\right]\left(e^{-\mu_a}\right) - I_{D_a}c_a}$$

Where.
$\frac{1}{\lambda_i} = \sum_{j=0}^{i}\frac{1}{p_j}$; if p_j are a function of age at disease onset then $\frac{1}{\lambda_{i,a}} = \sum_{j=0}^{i}\frac{1}{p_{j,a}}$
Then, disease onset rate at age a is estimated as

$$\theta_a = -\ln\left(1 - P_{H_aU_a}\right)$$

Step 2: Calculate prevalence of healthy state:

$$\pi_{H_a} = \frac{A_a - \sum_{k=0}^{a-1}\left(\pi_{H_k}P_{H_kU_k}P(T \geq a-k)P(S \geq a-k)\right)}{1 + P_{H_aU_a}};$$

$$P(T \geq a-k)P(S \geq a-k) = \sum_i s_i\left(1-e^{-(a-1-k)\lambda_i}\right)\prod_{j=k:a} e^{-\mu_j}$$

Where,
$\frac{1}{\lambda_i} = \sum_{j=0}^{i}\frac{1}{p_j}$; if p_j are a function of age at disease onset then $\frac{1}{\lambda_{i,a}} = \sum_{j=0}^{i}\frac{1}{p_{j,a}}$

Step 3: Increment a by 1; if a is less than the maximum age goes to step 1, else stop.

A.1.2. Estimation of diagnostic rates

In the second step of the two-step Markov process, for estimation of diagnostic rates, we reformulate the discrete-time Markov process $\boldsymbol{X}$, in previous section that defined disease onset and progression, into a continuous-time discrete-state Markov process $\boldsymbol{Y} = \{Y_t; t \geq 0, Z, \mathbb{Q}\}$, with more granular discretization of the state space as $Z = \{[H_a],[U_{i,a}],[D_{i,a}]\}$, for stage $i \in \{0 = CIS, 1 = Local, 2 = Regional, and\ 3 = Distant\}$ and age a, and rate matrix $\mathbb{Q}$. We estimated diagnostic rates in each stage of cancer, i.e., transition rates from preclinical to clinical states ($d_{i,a}$), by using a simulation-based optimization of the Markov process $\boldsymbol{Y}$.

The objective of the simulation-based optimization model is to minimize the sum of square errors between the simulated cancer incidence ($\overline{I_a}$) and the GLOBOCAN predicted incidence (I_a). (13) The details of the model are presented in (9), which were applied to sub-Saharan Africa and Southeast Asia regions using data from 2008 to 2012, when there was not much screening in these regions. However, in the case of Peru, certain populations underwent screening prior to 2012. Therefore, we modified the model in (9) to consider this difference, which we disucss here. For completeness, we first present the earlier version of the model formulation before discussing the modifications specific to Peru. The objective function was formulated as

$$Minimize_{d_{i,a}} \sum_a \left(\overline{I_a} - I_a\right)^2,\ d_{i,a} \geq 0,\ \forall i,a \qquad (4)$$

As the analytical form of $\overline{I_a}$ are unknown, we used a numerical optimization solution method where the objective function value can be evaluated numerically through simulation at any specific values of the decision parameters $d_{i,a} \geq 0, \forall i,a$. Here, for any specific $d_{i,a}$ values, we simulated the Markov Process $\boldsymbol{Y}$ over time t using $\boldsymbol{\rho}_{t+1} = \boldsymbol{\rho}_t + \boldsymbol{\rho}_t \mathbb{Q} \Delta t$ until it reached state steady, i.e.,

$$\boldsymbol{\rho} = \boldsymbol{\rho} + \boldsymbol{\rho} \mathbb{Q} \Delta t \tag{5}$$

where $\boldsymbol{\rho}$ is a vector of state distribution at steady state and $\mathbb{Q}$ is the rate matrix. We estimated $\overline{I_a}$ using $\overline{I_a} = \sum_i \rho_{U_{i,a}} d_{i,a}$, where $\rho_{U_{i,a}}$ is the steady state value for state $U_{i,a}$ (denoting the prevalence in pre-clinical cancer stage i at age a), which can be estimated by expansion of equation (5) as

$$\rho_{U_{i,a}} = \rho_{U_{i,a}} + \rho_{U_{i-1,a-1}} \lambda_{i-1,a} - \rho_{U_{i,a-1}} (\lambda_{i,a} + d_{i,a} + \mu_{i,a}) \tag{6}$$

In the previously presented model in (9), because of the assumption that diagnosis occurs only based on symptoms and that the probability of showing symptoms are higher in advanced disease stages, i.e., $d_{i,a} > d_{i-1,a}$, the distribution of the stage at diagnosis was a good approximation for the ratio of stage-specific diagnostic rates. That is, $\frac{d_{i,a}}{d_{3,a}} = \sum_{j=0}^{i} s_j$, where s_j is the proportion diagnosed in stage j, and $d_{i,a}$ is the diagnostic rate at state i and age a. Therefore, for the terms in the objective function in equation (4) we could write

$$\left(\overline{I_a} - I_a\right)^2 = \left(\sum_i \rho_{U_{i,a}} d_{i,a} - I_a\right)^2 = \left(\sum_i \rho_{U_{i,a}} \left(d_{3,a} \sum_{j=0}^{i} s_j\right) - I_a\right)^2 \approx f(d_{3,a}) \tag{7}$$

That is, the only unknown values in the objective function in equation (4) were the diagnostic rates in the last stage of cancer ($d_{3,a}$), as the steady state values in the pre-clinical states, $\rho_{U_{i,a}}$, are estimated numerically from the simulation of the Markov model in equation (5) as discussed above. The resulting objective function was

$$Minimize_{\ d_{3,a}} \sum_a \left(\sum_i \rho_{U_{i,a}} \left(d_{3,a} \sum_{j=0}^{i} s_j\right) - I_a\right)^2 \tag{8}$$

and the decision variables $d_{3,a} \forall a$ were solved iteratively for each a. However, in the case of Peru, certain populations have undergone screening based on recommendations prior to 2012 (the latest incidence data available at the time of this work was for year 2012), and thus, the assumption $d_{i,a} > d_{i-1,a}$ does not hold. Therefore, we modified the objective function in equation (7) to

$$Minimize_{\ d_{i,a}, \forall i,a} \sum_{i,a} \left(\rho_{U_{i,a}} (d_{i,a}) - I_a\right)^2,\ d_{i,a} \geq 0\ \forall i,a \tag{9}$$

that is, the number of decision variables (the unknown values) now increase to include diagnostic rates $d_{i,a}$ for each stage i and age a, as the actual rates of screening currently occurring in the population are unknown. This creates many decision variables. As the number of decision variables increases, ascertaining the convergence of a solution algorithm to the global optima becomes more challenging. We address this by showing below that the optimization problem in equation (9) is separable both on i and a and thus equation (9) can be converted to ia number of sub-problems. Each sub-problem can then be solved separately but iteratively for $d_{i,a}$, iterating over each i and a (see below). We further test for the convexity of each sub-problem (see Appendix C).

Remark 1: We can rewrite equation (9) as,

$$Minimize_{\ d_{i,a}} \left(\rho_{U_{i,a}} (d_{i,a}) - I_a\right)^2,\ d_{i,a} \geq 0 \tag{10}$$

for each combination of i,a pair thus generating ia number of sub-problems. Each function can then be solved separately for $d_{i,a}$ but iteratively over age a starting from the youngest age and, within each age, iteratively over cancer state i starting with the earliest disease state.

Proof:

Using the expression for $\rho_{U_{i,a}}$, from the expansion of the Markov process in equation (6) discussed above, and multiplying by $d_{i,a}$ we can write

$$\rho_{U_{i,a}} d_{i,a} = [\rho_{U_{i,a}} + \rho_{U_{i-1,a-1}} \lambda_{i-1,a} - \rho_{U_{i,a-1}} (\lambda_{i,a} + d_{i,a} + \mu_{i,a})] d_{i,a} \quad (11)$$

In equation (8), for $i = 0$ (the in-situ stage) $\lambda_{i-1,a-1} = \theta_{a-1}$ the cancer onset rate, and for all other values of i (i.e., local, regional, and distant stages) $\lambda_{i-1,a-1}$ are the progression rates (see Figure S1); and $\mu_{i,a-1}$ are the mortality rates. Values for $\lambda_{i-1,a-1}$ and $\mu_{i,a-1}$ are known. When $i = 0$ (the in-situ stage) $\rho_{U_{i-1,a-1}} = \rho_{H_{a-1}}$denoting the steady state value in healthy (i.e., prevalence of healthy stage), and under all other values of i, $\rho_{U_{i-1,a-1}}$ are the steady state values in the pre-clinical states (i.e., prevalence of pre-clinical cancer stages). For any given i,a pair, from Remark 2 and its proof below, the steady state values for $\rho_{U_{i,a-1}}$ and $\rho_{U_{i-1,a-1}}$, and solution to $d_{i,a-1}$ are known. Therefore, for any value of $d_{i,a}$, the steady state value for $\rho_{U_{i,a}}$ can be calculated through simulation of the Markov process in equation (5). As such, the only unknown value in equation (11) will then be $d_{i,a}$.

This completes the proof.

Remark 2: If we iteratively solve for $d_{i,a}$ using equation (11) by iterating over a and, within each a, iterate over i, then, for any given i,a pair, the steady state values for $\rho_{U_{i,a-1}}$ and $\rho_{U_{i-1,a-1}}$, and the solution to $d_{i,a-1}$ are known. Thus, the only unknown term in equation (11) is $d_{i,a}$

Proof:

We prove this by applying mathematical induction on equation (11)

For $i = 0$, $a = 1$,

$$\rho_{U_{0,1}} d_{0,1} = [\rho_{U_{0,1}} + \rho_{H_0}\theta_1 - \rho_{U_{0,0}} (\lambda_{0,a} + d_{0,a} + \mu_{H,a})] d_{0,1} \quad (12)$$

Then, the only unknown value is $d_{0,1}$ because $\rho_{U_{0,0}} = 0$ and ρ_{H_0} is the actual prevalence of healthy persons in age 0 (obtained from population demographics) as the first age for disease risk is 1, and all other parameters are known as discussed in proof of Remark 1.

Assuming the proof holds for $i = m$, $a = 1$,

for $= m + 1$, $a = 1$

$$\rho_{U_{m+1,1}} d_{m+1,1} = [\rho_{U_{m+1,1}} + \rho_{U_{m,0}} \lambda_{m,1} - \rho_{U_{m+1,0}} (\lambda_{m+1,1} + d_{m+1,1} + \mu_{m+1,1})] d_{m+1,1} \quad (13)$$

Then, the only unknown parameter is $d_{m+1,1}$ as $\rho_{U_{m,0}} = 0$ and $\rho_{U_{m+1,0}} = 0$ as the first age of disease risk is 1.

For $= 0$, $a = 2$

$$\rho_{U_{0,2}} d_{0,2} = [\rho_{U_{0,2}} + \rho_{H_1}\theta_2 - \rho_{U_{0,1}} (\lambda_{i,2} + d_{i,2} + \mu_{i,2})] d_{0,2} \quad (14)$$

Then, the only unknown parameter is $d_{0,2}$ because $\rho_{H_1} = \rho_{H_1} - \rho_{H_0}(\theta_1 + \mu_{H,1})$ can be estimated through steady state simulation of equation (5) and $\rho_{U_{0,1}}$ was estimated previously under $= 0$, $a = 1$.

Assuming the proof holds for $i = m + 1$, $a = 2$,

$$\rho_{U_{m+1,2}} d_{m+1,2} = [\rho_{U_{m+1,2}} + \rho_{U_{m,1}} \lambda_{m,2} - \rho_{U_{m+1,1}} (\lambda_{m+1,2} + d_{m+1,2} + \mu_{m+1,2})] d_{m+1,2} \quad (15)$$

Then, the only unknown parameter is $d_{m+1,2}$ as $\rho_{U_{m,1}}$ and $\rho_{U_{m+1,1}}$ were estimated above under $= m$, $a = 1$ and $i = m + 1$, $a = 1$, respectively

Finally, assuming the proof holds for any i and $a = k$,

for any i, and $a = k + 1$

$$\rho_{U_{i,k+1}} d_{i,k+1} = [\rho_{U_{i,k+1}} + \rho_{U_{i-1,k}} \lambda_{i-1,k+1} - \rho_{U_{i,k}} (\lambda_{i,k+1} + d_{i,k+1} + \mu_{i,k+1})] d_{i,k+1} \quad (16)$$

Then, the only unknown parameter is $d_{i,k+1}$ as $\rho_{U_{i-1,k}}$ and $\rho_{U_{i,k}}$ were estimated above under any i and $a = k$. This completes the proof.

A.2. Test for convexity of the optimization model for estimation of diagnostic rates

To check for the convergence of the solution to global optima we test for the convexity of the objective functions.

Specifically, we test for the commonly used convexity test, a function $f(x)$ that is twice differentiable on x is convex if it is positive semi-definite, i.e., the second derivative $f''(x) \geq 0$ at all points of x. However, we do not know the analytical form of $\bar{I}_{i,a}$ to calculate the second derivative of the objective function $(\bar{I}_{i,a} - I_{i,a})^2$. Therefore, for each combination of cancer stage (i) and age (a) pair, we empirically generated the function for $\bar{I}_{i,a}$ by estimation at multiple points of $d_{i,a}$. See Figure S1 and Figure S2 for results on In-situ and Local stages of cancer and at multiple age groups.

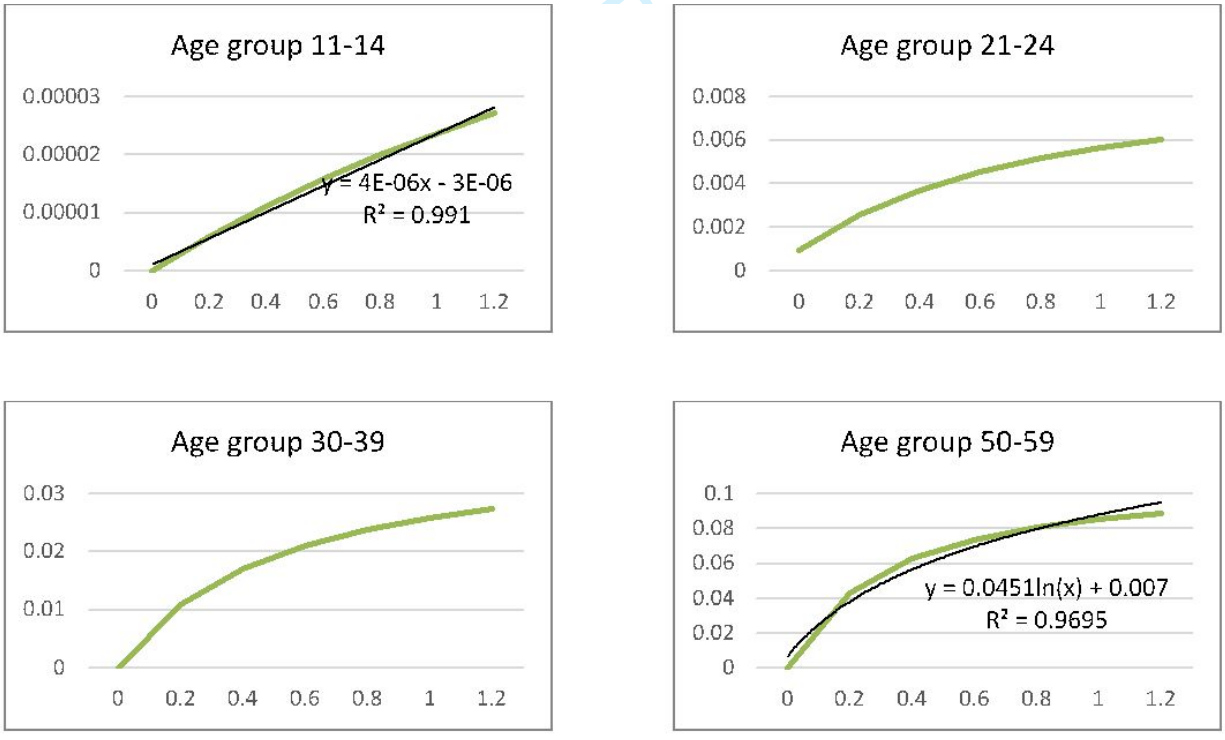

Figure S2: Incidence vs diagnostic rate for specific age-group and In-situ stage of cancer

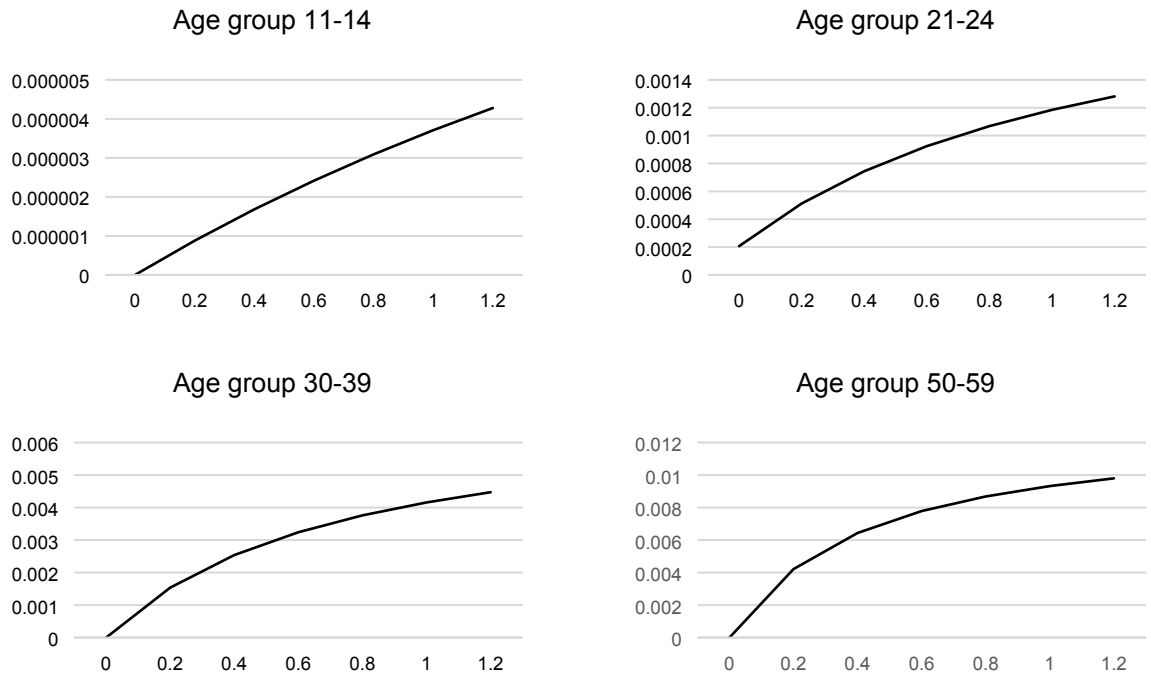

Figure S3: Incidence vs diagnostic rate for specific age-group and local stage of cancer

From the above empirical results, for any given cancer stage and age, the simulated incidence $\bar{I}_{i,a}$ is approximately a linear or a logarithmic function of diagnostic rates $d_{i,a}$, i.e.,

$\bar{I}_{i,a} \sim c\ ln\ (d_{i,a}) + b$ or $\bar{I}_{i,a} \sim c d_{i,a} + b$ for some constants c and b.

Writing $x = d_{i,a}$,

If $\bar{I}_{i,a} \sim c\ ln\ (x) + b$, the second derivative of the objective function $(\bar{I}_{i,a} - I_{i,a})^2$ on x is

$$f''(x) = \frac{d^2}{dx^2}(cln\ (x) + b - I_{i,a})^2 = \frac{2(I_{i,a} - b - cln\ (x) + c)}{x^2} > 0 \text{ as } I_{i,a} > b \quad (17)$$

And if $\bar{I}_{i,a} \sim cx + b$, the second derivative of the objective function $(\bar{I}_{i,a} - I_{i,a})^2$ on x is

$$f''(x) = \frac{d^2}{dx^2}(cx + b - I_{i,a})^2 = 2c(c) > 0 \quad (18)$$

thus, indicating that the objective function $(\bar{I}_{i,a} - I_{i,a})^2$ is convex.

A.3. Data assumptions for parameterization of cancer onset and progression for Peru

Table S3 presents data specific to the US and Peru that were used for constructing cancer onset and progression models specific to these countries using the two-step Markov process methodology discussed above in A.1

Table S3: Region specific input data for parameterization

Parameters	Value	Reference
GENERAL PROGRESSION PARAMETERS		(14) (15) (16)
Progression rates (average over age)		
In-situ to Local ($p_{0,.}$)	0.19	
Local to Regional ($p_{1,.}$)	0.33	
Regional to Distant ($p_{2,.}$)	0.43	
Distant to Death ($p_{3,.}$)	0.50	
Annual mortality rate (per woman year) without treatment by stage at diagnosis (average over age)		
In-situ ($\bar{\mu}_{0,.}$)	0.08	
Local ($\bar{\mu}_{1,.}$)	0.14	
Regional ($\bar{\mu}_{2,.}$)	0.23	
Distant($\bar{\mu}_{3,.}$)	0.50	
Annual mortality rate (per woman year) with treatment by stage at diagnosis (average over age)		
In-situ ($\bar{\bar{\mu}}_{0,.}$)	0.01	
Local ($\bar{\bar{\mu}}_{1,.}$)	0.02	
Regional ($\bar{\bar{\mu}}_{2,.}$)	0.08	
Distant ($\bar{\bar{\mu}}_{3,.}$)	0.27	
Note: Here '.' denotes the age		
REGION-SPECIFIC DATA		
Pre-screening incidence per 1000 women per year (I_a)		(17) (18)
Age group	Peru	US
0-14	0.00	
15-19	0.00	0.00
20-24	0.01	
25-29	0.05	0.09
30-34	0.14	0.26
35-39	0.36	0.58
40-44	0.70	1.09
45-49	0.91	1.72
50-54	1.05	1.97
55-59	1.38	2.21
60-64	1.38	2.60
65-69	1.52	2.84
70-74	1.52	3.06
75-79	1.56	3.33

80-84	2.16	3.43	
85+	2.14		
Distribution of stage at diagnosis in base-case			(18) (19) (20) (21)
Stage	Peru	US	
In-Situ (s_0)	3%	4.70%	
Local (s_1)	43%	48.30%	
Regional (s_2)	45%	39.50%	
Distant (s_3)	9%	7.50%	

B. Markov decision process (MDP) to identify optimal screening schedules for mammography

B.1. Formulation of the problem of identifying optimal screening schedule as a MDP model

The parameterized cancer onset and progression model from section A was used in a Markov decision process model to identify an optimal screening schedule. Specifically, we formulated the problem as a finite-state, finite-horizon and discrete-time MDP defined by a 6-tuple $\{Y_t, D_t; Z, S, \mathbb{P}_s, R_s\}$, where $t = \{1,2,3 \ldots, 100\}$ are the decision-making stages; here, stages represent individual ages, i.e., $t = a$, therefore, for convenience, we will use 'age' to refer to the normally used terminology of 'stage' in MDP models, replacing t with a,

$Y_a \epsilon$ Z is the disease state at age a, defined over the state space $\mathrm{Z} = \{[H_a],[U_{i,a}],[D_{i,a}],M\}$, where $[H_a]$,$[U_{i,a}]$, $[D_{i,a}]$ are healthy, preclinical, and clinical states in disease stage $i \in \{0 = CIS, 1 = Local, 2 = Regional, and\ 3 = Distant\}$ and age a, as in the Markov process model in the previous section, and M denotes a mortality state,

S is the action space which is a set of possible decision choices, here we have 2 possible choices, i.e., $S = \{Screen(1), Do\ not\ Screen(0)\}$

$D_a \epsilon\ S$ is the decision taken at age a (choosing from set S),

$\mathbb{P}_s$ is the transition probability matrix corresponding to action s, specifically, each element $p(i',a,s,j)$ of the matrix $\mathbb{P}_s$ represents the probability of transitioning from state i' to state j if the person is at age a and action s is taken, and

R_s is the immediate reward matrix corresponding to action s, specifically, each element $r(i',a,s,j)$ of matrix R_s represents the immediate reward of taking action s when the person is in state i' at age a and as a result the person transitions to state j.

The problem is then to solve for the optimal values of D_a. Use of MDP in this context has been studied before, (22) so we do not discuss further details of the methodology here. We only show the formulation of the problem in the context of identifying optimal screening schedules for mammography considering costs of screening and monetary value per quality-adjusted life-year lived.

The above MDP was solved using dynamic programming, which is formulated as follows.

Let $V(i',a,s)$ be the value of choosing action s when the system is in state i' at age a,

$$V(i',a,s) = \sum_{i' \in k} \left(\frac{\rho_{i'}}{\sum_{m \in k} \rho_m} \right) \left[\sum_{j \in Z} p(i',a,s,j) r(i',a,s,j) + \sum_{j \in Z} p(i',a,s,j) J^*(i',a+1) \right]$$
$$\forall s \in S, \forall\ i' \in k = \{[H_a],[U_{i,a}]\} \quad (19)$$

where,

$$J^*(i',a) = r(i',a,s^*(i',a)) + \sum_{j \in Z} p(i',a,s^*(i',a),j) J^*(i',a+1) \quad (20)$$

Then, the optimal decision $s^*(i',a)$ at age a and disease state i'can be written as

$$s^*(i',a) = \begin{cases} arg\ max_{s \in S}\ V(i',a,s)\ , if\ i' = k = \{[H_a],[U_{i,a}]\}, \\ Do\ nothing, if\ i' \epsilon \{[D_{i,a}],M\} \end{cases} \quad (21)$$

Note that, with the above equations, all states in $= \{[H_a],[U_{i,a}]\}$, will have the same optimal action because, in the absence of diagnosis, we cannot distinguish between persons in preclinical cancer states $[U_{i,a}]$ from healthy state $[H_a]$. For persons in states$[D_{i,a}]$ and M, i.e., for persons in clinical cancer states and deaths, respectively, the action is to do nothing.

Transition probabilities, $p(i',a,s,j)$, are estimated using the parameterized model from section A. The specific equations are presented in Tables S4, S5, and S6. Immediate rewards incorporate the costs and benefits of screening as follows.

$$r(i',a,s = no\ screening,j) = \begin{cases} 0, if\ j\ is\ mortality \\ r_{LY}.q_j + c_d + c_i, if i' \in [U_{i,a}]\ and\ j \in [D_{i,a}] \\ r_{LY}.q_j + c_t, if i' \in [D_{i,a}]\ and\ j \in M \\ r_{LY}.q_j\ otherwise \end{cases}, \text{and} \quad (22)$$

$$r(i',a,s = screening,j) = \begin{cases} 0\ if\ j\ is\ mortality \\ r_{LY}.q_j + c_d + c_i, if\ i' \in [U_{i,a}]\ and\ j \in \{[D_{i,a}]\} \\ r_{LY}.q_j + c_t, if i' \in [D_{i,a}]\ and\ j \in M \\ r_{LY}.q_j + c_s\ otherwise \end{cases} \quad (23)$$

where,

$c_s = -\left(\zeta_{mammography_a} c_{mammogram} + (1 - \zeta_{mammography_a})(c_{mammogram} + c_{-diagnosis})\right)$,

$c_d = -\left(c_{mammogram} + c_{+diagnosis}\right)$,

$r_{LY} =$ value-per-QALY lived,

q_j= QALY associated with state j, $q_j = \begin{cases} 1\ if\ j = H_a \\ 0\ if\ j = M \\ 0 < q_j < 1\ otherwise \end{cases}$, (24)

$\zeta_{mammography_a}$ is the specificity of mammography at age a,

$c_{mammogram}$ is the unit cost of mammography per person,

$c_{-diagnosis}$ is the cost of follow-up diagnostic tests for a false positive (per person)

$c_{+diagnosis}$ is the cost of follow-up diagnostic tests for a true positive (per person)

c_i is the initial treatment cost per person,

c_t is terminal treatment cost per person, which was applied at the final year of life for women who die from breast cancer.

Table S4: Notation used in transition probability matrix

$\theta_{i,a}$	Onset rate of breast cancer
$\lambda i,a$	Dwell rate for cancer stage i and age a
$d_{i,a}$	Diagnostic rate of cancer in stage i and age a
μ_a	Natural mortality rate at age a
$\mu_{i,a}$	Diseased mortality in cancer stage i and age a

Table S5: Transition probability matrix for action = no screening

$$
\begin{bmatrix}
e^{-\mu_a}\left(\frac{1}{\theta_a+1}\right) & e^{-\mu_a}\left(\frac{\theta_a}{\theta_a+1}\right) & 0 & 0 & 0 & 0 & 0 & 1-e^{-\mu_a} \\
0 & e^{-\mu_a}\left(\frac{1}{d_{0,a}+\lambda_{0,a}+1}\right) & e^{-\mu_a}\left(\frac{\lambda_{0,a}}{d_{0,a}+\lambda_{0,a}+1}\right) & 0 & e^{-\mu_a}\left(\frac{d_{0,a}}{d_{0,a}+\lambda_{0,a}+1}\right) & 0 & 0 & 1-e^{-\mu_a} \\
0 & 0 & e^{-\mu_a}\left(\frac{1}{d_{1,a}+\lambda_{1,a}+1}\right) & e^{-\mu_a}\left(\frac{\lambda_{1,a}}{d_{1,a}+\lambda_{1,a}+1}\right) & 0 & e^{-\mu_a}\left(\frac{d_{1,a}}{d_{1,a}+\lambda_{1,a}+1}\right) & 0 & 1-e^{-\mu_a} \\
0 & 0 & 0 & e^{-\mu_a}\left(\frac{1}{d_{2,a}+\lambda_{2,a}+1}\right) & e^{-\mu_a}\left(\frac{\lambda_{2,a}}{d_{2,a}+\lambda_{2,a}+1}\right) & 0 & e^{-\mu_a}\left(\frac{d_{2,a}}{d_{2,a}+\lambda_{2,a}+1}\right) & 1-e^{-\mu_a} \\
0 & 0 & 0 & 0 & e^{-(\mu_a+\bar{\mu}_{0,a})} & 0 & 0 & 1-e^{-(\mu_a+\bar{\mu}_{0,a})} \\
0 & 0 & 0 & 0 & 0 & e^{-(\mu_a+\bar{\mu}_{1,a})} & 0 & 1-e^{-(\mu_a+\bar{\mu}_{1,a})} \\
0 & 0 & 0 & 0 & 0 & 0 & e^{-(\mu_a+\bar{\mu}_{2,a})} & 1-e^{-(\mu_a+\bar{\mu}_{2,a})} \\
0 & 0 & 0 & 0 & 0 & 0 & 0 & 1-e^{-(\mu_a+\bar{\mu}_{3,a})} \\
0 & 0 & 0 & 0 & 0 & 0 & 0 & 1
\end{bmatrix}
$$

Table S6: Transition probability matrix for action = screening

$$
\begin{bmatrix}
e^{-\mu_a}\left(\frac{1}{\theta_a+1}\right) & e^{-\mu_a}\left(\frac{\theta_a}{\theta_a+1}\right) & 0 & 0 & 0 & 0 & 0 & 1-e^{-\mu_a} \\
0 & e^{-\mu_a}\left(\frac{s}{\bar{d}_{0,a}+\bar{\lambda}_{0,a}+s}\right) & e^{-\mu_a}\left(\frac{\bar{\lambda}_{0,a}}{\bar{d}_{0,a}+\bar{\lambda}_{0,a}+s}\right) & 0 & 0 & 0 & 0 & 1-e^{-\mu_a} \\
0 & 0 & e^{-\mu_a}\left(\frac{s}{\bar{d}_{1,a}+\bar{\lambda}_{1,a}+s}\right) & e^{-\mu_a}\left(\frac{\bar{\lambda}_{1,a}}{\bar{d}_{1,a}+\bar{\lambda}_{1,a}+s}\right) & 0 & 0 & 0 & 1-e^{-\mu_a} \\
0 & 0 & 0 & e^{-\mu_a}\left(\frac{s}{\bar{d}_{2,a}+\bar{\lambda}_{2,a}+s}\right) & e^{-\mu_a}\left(\frac{\bar{\lambda}_{2,a}}{\bar{d}_{2,a}+\bar{\lambda}_{2,a}+s}\right) & 0 & 0 & 1-e^{-\mu_a} \\
0 & 0 & 0 & 0 & e^{-\mu_a}\left(\frac{s}{\bar{d}_{3,a}+s}\right) & e^{-\mu_a}\left(\frac{\bar{d}_{3,a}}{\bar{d}_{3,a}+s}\right) & 1-e^{-(\mu_a+\bar{\lambda}_{3,a})} & 1-e^{-(\mu_a+\bar{\lambda}_{3,a})} \\
0 & 0 & 0 & 0 & e^{-(\mu_a+\bar{\bar{\mu}}_{0,a})} & 0 & 1-e^{-(\mu_a+\bar{\bar{\mu}}_{0,a})} & 1-e^{-(\mu_a+\bar{\bar{\mu}}_{0,a})} \\
0 & 0 & 0 & 0 & 0 & e^{-(\mu_a+\bar{\bar{\mu}}_{1,a})} & 1-e^{-(\mu_a+\bar{\bar{\mu}}_{1,a})} & 1-e^{-(\mu_a+\bar{\bar{\mu}}_{1,a})} \\
0 & 0 & 0 & 0 & 0 & e^{-(\mu_a+\bar{\bar{\mu}}_{2,a})} & 1-e^{-(\mu_a+\bar{\bar{\mu}}_{2,a})} & 1-e^{-(\mu_a+\bar{\bar{\mu}}_{2,a})} \\
0 & 0 & 0 & 0 & 0 & 0 & e^{-(\mu_a+\bar{\bar{\mu}}_{3,a})} & 1-e^{-(\mu_a+\bar{\bar{\mu}}_{3,a})} \\
0 & 0 & 0 & 0 & 0 & 0 & 0 & 1
\end{bmatrix}
$$

Where,

$\overline{d}_{i,a} = (1 - \eta_{mammography})d_{i,a} + \eta_{mammography} - \eta_{mammography}(1 - \eta_{mammography})d_{i,a}$

$\overline{\lambda}_{i,a} = (1 - \eta_{mammography})\lambda_{i,a}$

$s = (1 - \eta_{mammography})$

B.2. Data assumptions used for the MDP model

Country-specific data related to the natural cancer progression, specifically the transition probability matrices in Tables S5 and S6, are the same data used in the two-step Markov process methodology and are listed in Table S3. Data related to mammography (film) screening are presented in Table S7. We assumed the use of film mammography in Peru as the availability of digital mammography is limited in developing countries (23). We used data f from the Breast Cancer Surveillance Consortium (BCSC) presented in (24). Further, as mammography sensitivity and specificity varied by breast density, we used weighted average values, weighted by the proportion of persons presenting with the different breast density as reported in the BCSC.

Table S7: Parameters specific to screen-film mammography

Parameter name	**Assumption** (25) (26) (24) (27)				
$\zeta_{mammography}$ (Specificity of film mammogram) for Peru and US (24), (27)	Age	Initial	Annual	Biennial	Triennial
	<29	0.83000	0.83000	0.83000	0.83000
	30-34	0.85800	0.85800	0.85800	0.85800
	35-39	0.87500	0.87500	0.87500	0.87500
	40–49	0.85356	0.91812	0.90472	0.89606
	50-59	0.85576	0.91974	0.90498	0.90013
	60-69	0.86576	0.92974	0.91459	0.91013
	70-79	0.88384	0.93602	0.92127	0.91974
$\eta_{mammography}$ (Sensitivity of film mammogram) for Peru and US (24), (27)	Age	Initial	Annual	Biennial	Triennial
	<29	0.66700	0.66700	0.66700	0.66700
	30-34	0.81500	0.81500	0.81500	0.81500
	35-39	0.76100	0.76100	0.76100	0.76100
	40–49	0.87158	0.75644	0.8173	0.83026
	50-59	0.88126	0.77184	0.82155	0.83783
	60-69	0.90754	0.80298	0.85269	0.86897
	70-79	0.92611	0.84373	0.88126	0.8964
$\zeta_{mammography}$ (Specificity of film mammogram) for US validation (28)	Age	Specificity			
	<40	0.906			
	40-44	0.906			
	45-49	0.904			
	50-54	0.916			
	55-59	0.922			
	60-64	0.925			
	65-69	0.93			
	70-74	0.937			
	75-89	0.942			

$\eta_{mammography}$ (Sensitivity of film mammogram) for US validation and Peru sensitivity analysis (28), (29)	Age: Sensitivity <40: 0.55 40-44: 0.645 45-49: 0.701 50-54: 0.744 55-59: 0.744 60-64: 0.744 65-69: 0.744 70-74: 0.798 75-89: 0.807
$\zeta_{mammography}$ (Specificity of film mammogram) for Peru sensitivity analysis (28)	Age: Specificity <40: 0.841 40-44: 0.841 45-49: 0.823 50-54: 0.816 55-59: 0.84 60-64: 0.856 65-69: 0.86 70-74: 0.869 75-89: 0.88
c_{screen} (Screening cost) for Peru (12)	2.45 USD
c_{screen} (Screening cost) for US (24)	81.35 USD
$c_{diagnosis}$ (Cost of follow-up tests if diagnosed) for Peru (12)	True positive, $: 551.36; False positive, $: 72.18
$c_{diagnosis}$ (Cost of follow-up tests if diagnosed) for US (24)	Age group: True positive, $; False positive, $ 40–49: 2187.89; 229.1612 50–64: 2053.74; 271.6121 65–74: 2065.13; 272.353 ≥75: 1741.3; 280.5171
$c_{treatment}$ (Cost of treatment by stage at diagnosis) for US (24)	Stage: Initial, $; Terminal, $ In situ: 13055; 35335 localized: 13055; 35335 Regional: 24682; 41825 Distant: 38119; 58665
$c_{treatment}$ (Cost of treatment by stage at diagnosis) for Peru (12) for initial cost; proportion of terminal to initial cost for US used in calculation of terminal cost for Peru	Stage: Initial, $; Terminal, $ In situ: 218.01; 590 localized: 218.01; 590 Regional: 464.58; 787 Distant: 684.84; 1053
q_j= quality-adjusted life-years associated with state j	$q = [1, 1, 1, 1, 1, 0.992, 0.992, 0.971, 0.46, 0]$ corresponding to stage $[H_a, U_{in-situ}, U_{local}, U_{regional}, U_{distant}, D_{in-situ}, D_{local}, D_{regional}, D_{distant}, M]$

C. Model verification on the US population

C.1. Verifying parameterization of natural history model for the US

We verified that our model outputs match data or results observed in the CISNET study models, specifically the cumulative risk by age of cancer onset, and incidence of cancers by age and stage at diagnosis.

Table S8: Cumulative probability of onset of cancer by age

Age	US Study (2)	Estimations from our model
20	0.000	0.001
25	0.002	0.003
30	0.005	0.007
35	0.021	0.019
40	0.046	0.046
45	0.105	0.099
50	0.169	0.172
55	0.233	0.258
60	0.328	0.354
65	0.436	0.457
70	0.563	0.563
75	0.707	0.670
80	0.852	0.799
85	1.000	1.000

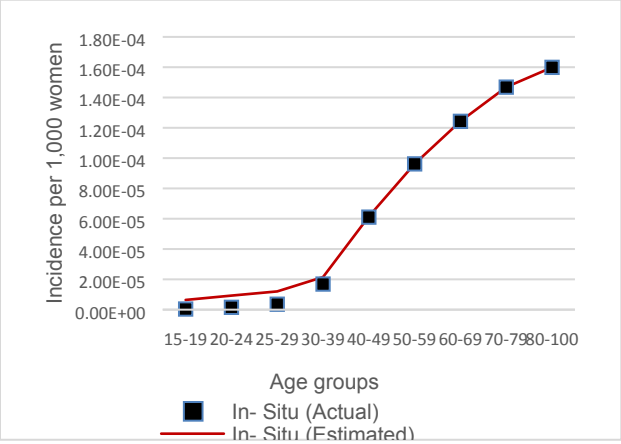

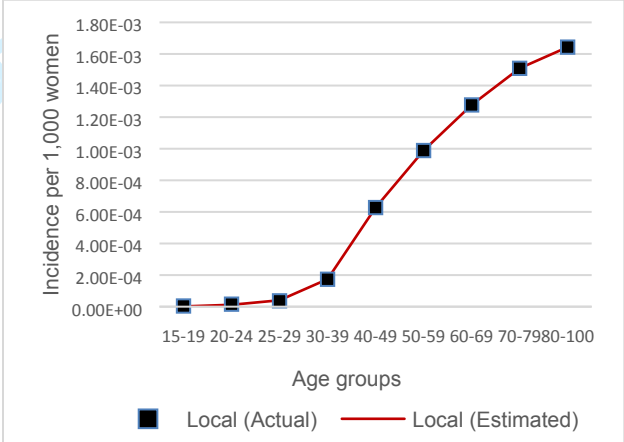

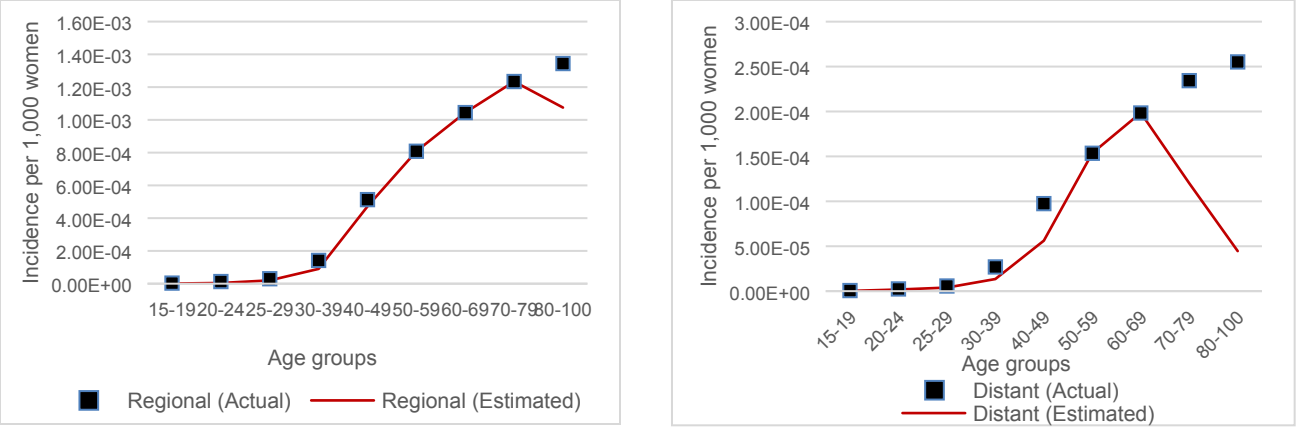

Figure S4: Comparison of estimated versus actual incidence by age and stage at diagnosis for US

C.2. Model validation on the US population

Results and analysis from our model related to mammography screening were compared with results from the CISNET study. Details of the analysis related to Figures S5, S6, and S7, and Table S8 are discussed in the main paper, under Validation section. All metrics are undiscounted.

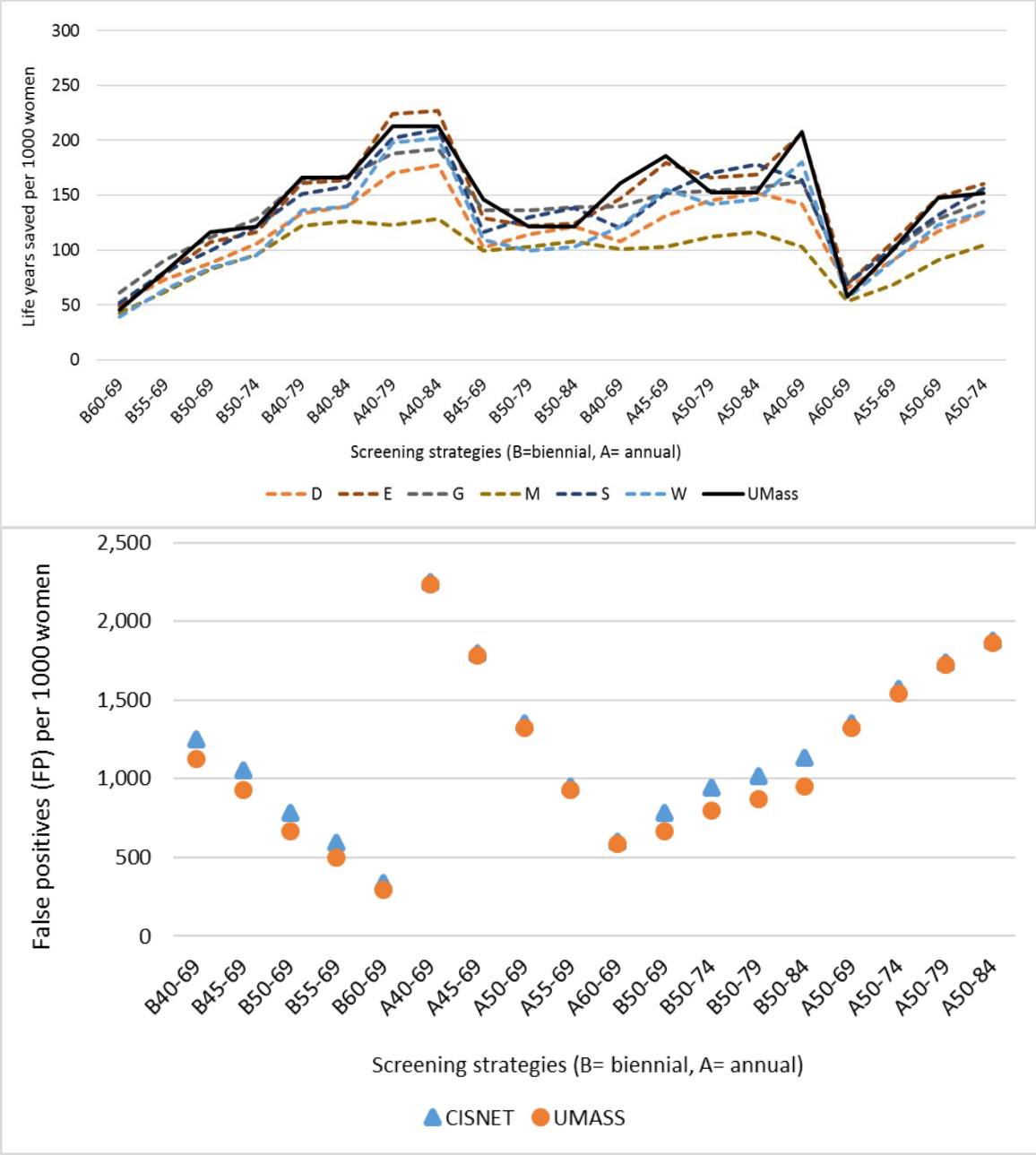

Figure S5: Model validation on the US population: Comparing benefits (life years saved per 1000 women) and harms (false positives) between our model (UMass) and CISNET model estimations. The x-axis presents the different screening strategies, biennial (B) or annual (A), and ages to screen. CISNET model group abbreviations: D = Dana-Farber Cancer Institute; E = Erasmus Medical Center; G = Georgetown University; M = M.D. Anderson Cancer Center; S = Stanford University; W = University of Wisconsin/Harvard.

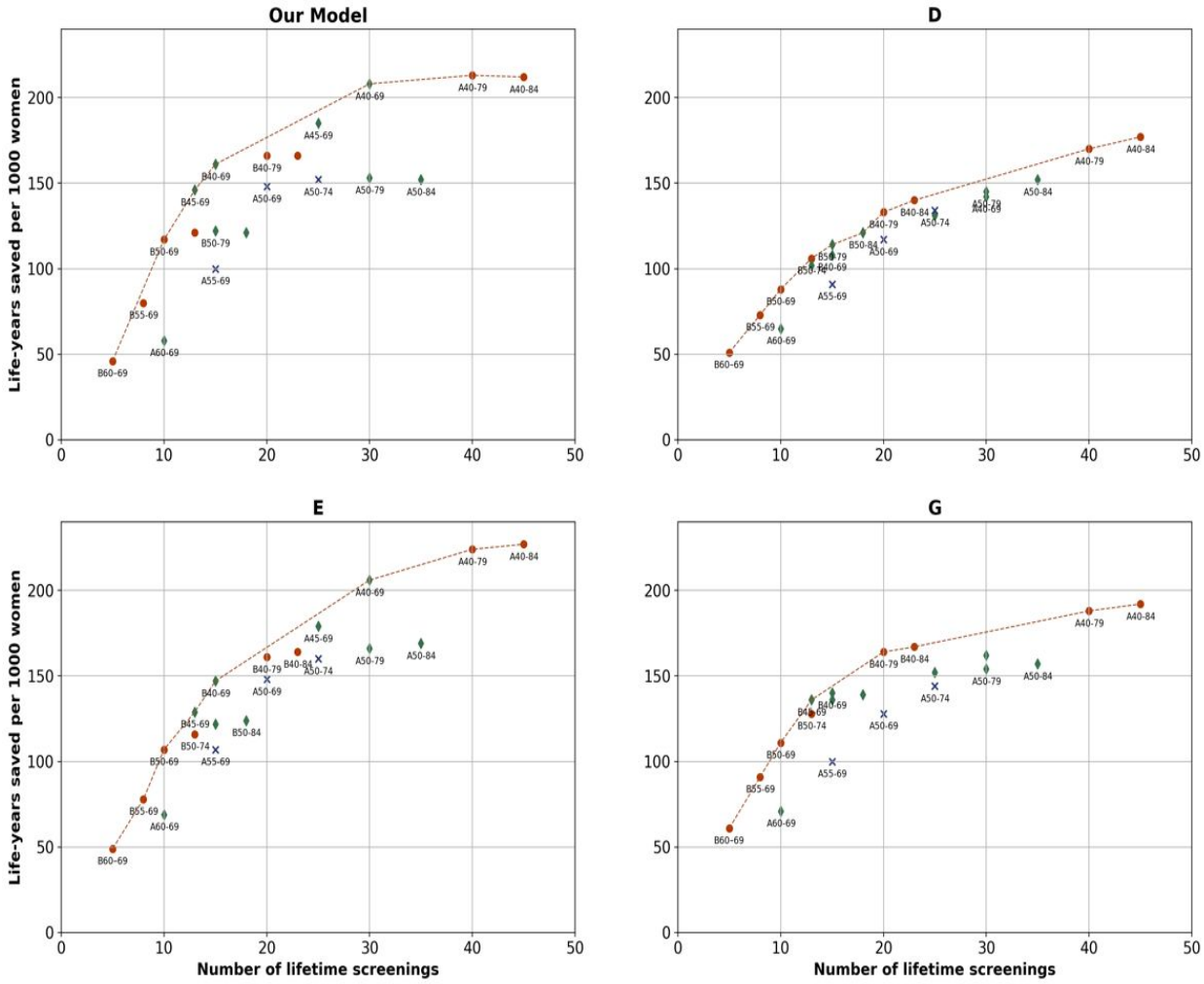

Figure S6: Comparing efficiency frontiers from our model with 3 CISNET models for pre-selected scenarios evaluated in the CISNET study for the US population. All metrics are undiscounted.

Figure legend: In the CISNET study, the screening schedules with red full circles were categorized as efficient (non-dominated in at least 5 CISNET models), scenarios in green diamond were categorized as borderline (dominated in 2-4 models), and the scenarios in blue "cross" were categorized as inefficient (dominated in all the models); Model Group Abbreviations: D (Dana Farber Cancer Center), E (Erasmus Medical Center), G (Georgetown U); B= biennial screening, A=annual screening

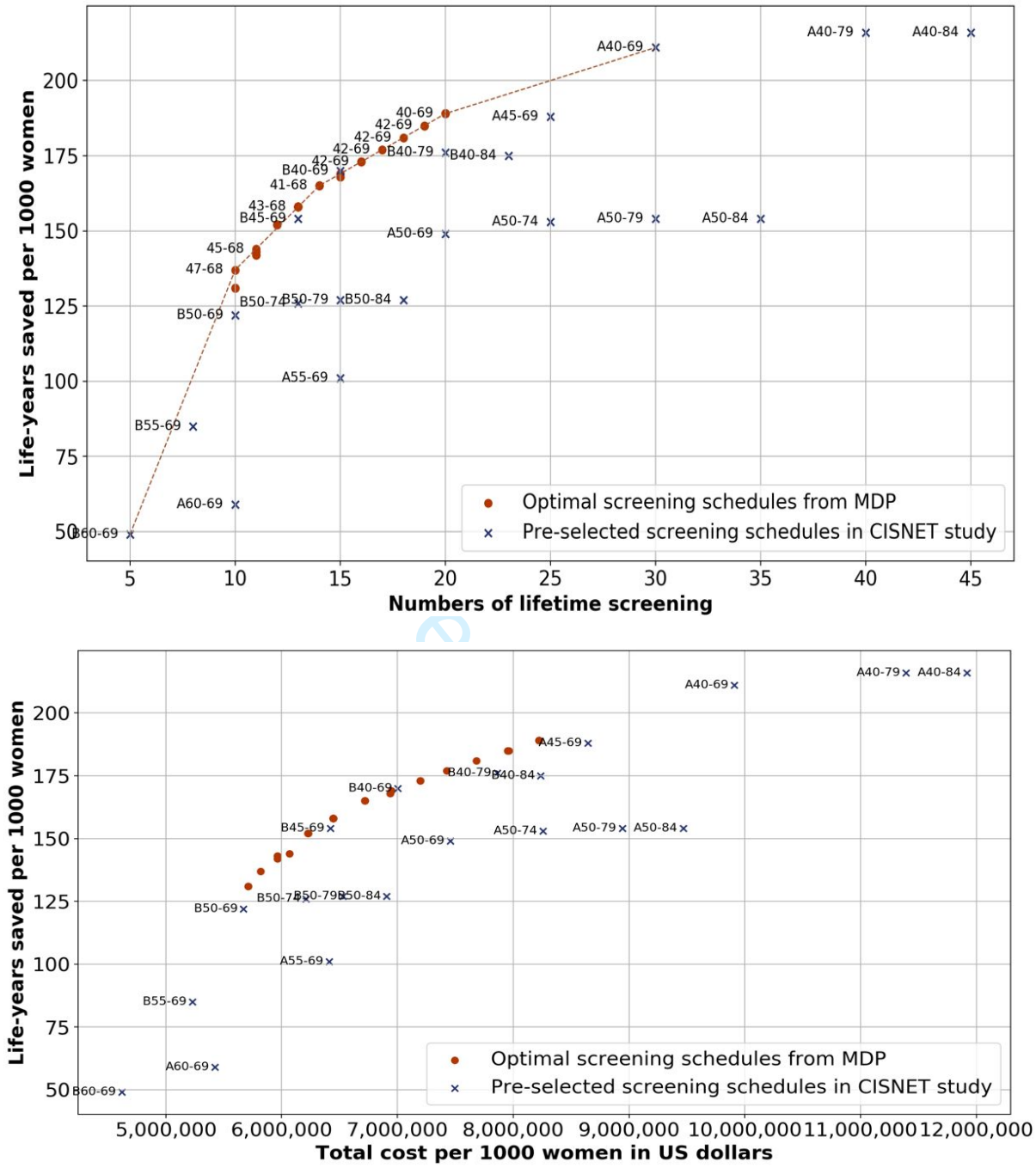

Figure S7: Efficiency frontier plotted by combining pre-selected scenarios in CISNET study with optimal scheduled generated by the model for the US population. All metrics are undiscounted.

Table S9: Benefits, harms, and costs under alternative screening schedules for the US.

Number of lifetime screenings	Age interval for screening	False positives per 1000 women	Life-years saved per 1000 women	QALYs saved per 1000 women	Total cost per 1000 women (undiscounted) (USD)	Cost per life-year saved (USD)	Cost per QALY saved (USD)
0	NA	NA	reference	reference	3,730,421	reference	reference
5 (B60-69)	60-69	388	49	69.23491	4,618,171	18,254	12,830
8 (B55-69)	55-69	636	85	114.9399	5,227,876	17,630	13,028
10	47-68	841	132	167.7138	5,710,988	15,099	11,806
11	45-68	931	142	180.5029	5,963,972	15,775	12,374
12	44-68	1022	152	190.8303	6,225,760	16,424	13,072
13	43-68	1097	158	197.9314	6,443,835	17,220	13,705
14	41-68	1190	165	205.5111	6,720,099	18,111	14,543
15	41-69	1264	168	209.3046	6,938,201	19,143	15,321
16	41-69	1349	173	215.6531	7,195,497	20,000	16,062
17	42-69	1437	177	220.4828	7,427,262	20,842	16,761
18	40-69	1513	181	224.1628	7,681,212	21,887	17,618
19	40-69	1600	185	229.3496	7,952,445	22,857	18,440
20	40-69	1693	189	233.9974	8,222,971	23,710	19,192

Note: Costs and benefits are undiscounted

D. Sensitivity analysis

D.1. Impact of mammography sensitivity and specificity

In the base case results presented in the main manuscript, we assumed the use of film mammography in Peru, as the availability of the more advanced digital mammography in developing countries is limited (23). Estimates from the breast cancer surveillance consortium (BCSC) suggests that mammography sensitivity and specificity have been increasing over time, representing the advancements in diagnostic tools. Therefore, we used mammography specificity and sensitivity from the 1995-1999 era (presented in Table S7) to test the impact of the unavailability of the most recent technology and human expertise. The results are presented in Table S10 below and discussed in the main manuscript.

Table S10: Sensitivity analysis using lower values of mammography test sensitivity and specificity- Comparison of model outputs between basecase and sensitivity analysis case for Peru

Number of lifetime screenings	Age interval for screening (base case)	Age interval for screening	False positives per 1000 women (base case)	False positives per 1000 women	Life-years saved per 1000 women (base case)	Life-years saved per 1000 women	QALYs saved per 1000 women	Total cost per 1000 women (undiscounted) (USD) (base case)	Total cost per 1000 women (undiscounted) (USD)	Cost per life-year saved (USD) (base case)	Cost per life-year saved (USD)	Cost per QALY saved (USD)
0	NA	NA	NA	NA	reference	reference	reference	52,644	46,967	reference	reference	reference
1	51-51	51-51	129	168	19	16	19	135,788	153,307	4,376	6,535	5,670
2	50-56	50-57	220	310	31	28	32	192,122	243,310	4,499	7,116	6,081
3	46-57	47-58	315	469	44	38	44	252,467	344,421	4,541	7,925	6,825
4	45-60	46-60	395	619	54	47	54	303,885	439,667	4,653	8,416	7,275
5	44-61	44-61	489	743	62	55	63	363,927	518,721	5,021	8,628	7,530
7	41-62	42-62	676	1,069	78	69	78	484,359	725,455	5,535	9,887	8,698
8	42-63	42-63	766	1,212	84	75	85	542,360	816,670	5,830	10,312	9,094
9	42-64	42-63	842	1,362	88	80	90	591,269	912,208	6,121	10,865	9,593
10	41-64	41-64	939	1,507	95	84	95	654,089	1,004,946	6,331	11,350	10,060
11	42-65	42-65	978	1,644	99	89	100	680,196	1,091,992	6,339	11,791	10,447
12	41-66	42-65	1,055	1,765	101	91	103	730,554	1,169,479	6,712	12,311	10,885
13	40-66	40-66	1,132	1,914	105	96	108	780,415	1,264,450	6,931	12,640	11,251
14	41-67	41-66	1,213	2,091	107	99	111	832,693	1,376,901	7,290	13,446	11,948
15	40-67	40-66	1,302	2,240	112	103	115	890,442	1,472,028	7,480	13,856	12,361
16	40-67	40-67	1,389	2,360	114	105	118	946,532	1,549,028	7,841	14,323	12,762
17	40-67	40-67	1,477	2,528	117	108	121	1,003,876	1,655,689	8,130	14,944	13,330

Note: Costs and benefits are undiscounted

D.2. Impact of dwell-times (inverse of progression rates)

As our model is deterministic, to test the impact of uncertainty in dwell times (inverse of progression rates between preclinical disease stages) on results for optimal screening schedules, we generated 100 runs of the model by sampling for different values of dwell times between the ranges presented in the Table S11. To ensure that progression in advanced stages of cancer are more aggressive than earlier stages, we sample using the following equation. Dwell time in stage $i = LR_i + \mathrm{x} * (UR_i - LR_i)$ where $\mathrm{x} = 1, 2, 3, 4, 5 \ldots\ldots\ldots 100$

We present the results in Table S12 and S13 below and discuss the findings in Results and Discussion sections of the main manuscript.

Table S11: Data assumptions for sensitivity analysis on dwell-times (inverse of progression rates)

Stage, i	Lower range (LR) (14)	Upper range (UR) (14)
DCIS	4.50	5.50

Local	2.50	3.76
Regional	1.54	3.10
Distant	1.50	2.50

Table S12: Sensitivity analysis on dwell-times- Comparing age interval, false positives per 1000 women, life-years (LY) saved per 1000 women and QALYs saved per 1000 women between basecase and sensitivity analysis case

	Age interval for screening			False positives per 1000 women			Life years saved per 1000 women			QALYs saved per 1000 women		
Dwell time range	Basecase	Lower	Upper	Basecase	Lower range	Upper range	Basecase	Lower range	Upper range	Basecase	Lower range	Upper range
No screening	–	–	–	reference	reference	reference	reference	reference	reference	reference	reference	reference
1	51-51	53-53	51-51	129	130	131	19	20	16	22	23	19
2	50-56	50-57	45-53	220	220	227	31	35	28	37	40	32
3	46-57	47-60	46-56	315	303	316	44	48	38	51	55	44
4	45-60	45-61	42-57	395	393	414	54	61	47	62	69	53
5	44-61	44-62	42-58	489	487	504	62	71	54	72	80	62
6	44-62	46-64	43-60	579	556	587	70	78	61	80	88	69
7	41-62	44-64	40-61	676	655	680	78	89	67	89	100	75
8	42-63	44-65	42-62	766	742	765	84	96	71	95	107	80
9	42-64	42-65	41-62	842	838	862	88	104	76	101	115	86
10	41-64	42-66	40-63	939	925	957	95	110	80	107	122	91
11	42-65	43-67	41-64	978	954	977	99	114	82	112	126	93
12	41-66	42-67	40-65	1,055	1,041	1,062	101	120	86	115	132	97
13	40-66	41-68	39-65	1,132	1,124	11,44	105	125	89	119	137	99
14	41-67	41-69	38-65	1,213	11,89	1,215	107	129	91	122	140	103
15	40-67	40-70	40-66	1,302	1,273	1,308	112	132	93	129	146	105

Note: Costs and benefits are undiscounted

Table S13: Sensitivity analysis on dwell-times- Comparing cost per LY saved, cost per QALY saved and cost per 1000 women between basecase and sensitivity analysis case

	Total cost per 1000 women, USD			Cost per life years saved per 1000 women, USD			Cost per QALY saved per 1000 women, USD		
Dwell time range	Basecase	Lower range	Upper range	Basecase	Lower range	Upper range	Basecase	Lower range	Upper range
No screening	reference	reference	reference	reference	reference	reference	reference	reference	reference
1	135,788	138,523	132,950	4,376	4,077	5,234	3,825	3,565	4,451
2	192,122	195,377	194,078	4,499	3,919	5,093	3,805	3,433	4,452
3	252,467	248,101	250,589	4,541	3,990	5,340	3,940	3,506	4,613
4	303,885	306,188	313,215	4,653	4,100	5,640	4,056	3,644	4,955
5	363,927	365,741	371,392	5,021	4,333	5,906	4,334	3,866	5,161
6	421,727	410,840	424,724	5,273	4,559	6,165	4,593	4,024	5,407
7	484,359	473,560	484,411	5,535	4,674	6,527	4,877	4,184	5,762
8	542,360	529,842	539,647	5,830	4,942	6,928	5,158	4,425	6,089
9	591,269	591,351	601,758	6,121	5,151	7,291	5,342	4,644	6,440
10	654,089	647,777	663,087	6,331	5,386	7,637	5,609	4,861	6,772
11	680,196	667,839	677,671	6,339	5,379	7,617	5,627	4,851	6,737
12	730,554	723,637	732,651	6,712	5,569	7,939	5,896	5,042	7,040
13	780,415	777,678	787,631	6,931	5,791	8,261	6,099	5,254	7,453
14	832,693	831,718	832,472	7,290	6,012	8,556	6,412	5,538	7,613
15	890,442	874,706	892,507	7,480	6,191	9,045	6,640	5,623	8,032

Note: Costs and benefits are undiscounted

D.3. Impact of uncertainty in carcinoma in-situ (CIS) pathways

Recent studies, under the context of over-diagnosis of cancers, have highlighted the uncertainty around pathways of CIS stage and mammography sensitivity for diagnosis at this stage, and their corresponding impact on the CIS progression rate estimates. (30), (31), (32), (33), (34), (35), (36)Therefore, as uncertainty analysis, we evaluated 5 CIS Cases (Table S14), each using different combinations of values for CIS progression rate, proportion of invasive cancers initiating directly in local stage, and mammography sensitivity in CIS stage. We present results for Peru and the US below in Figures S8 and S9. We present the observations and discuss the findings in Results and Discussion sections of the main manuscript.

Table S14: Scenarios for uncertainty analysis of CIS pathway

Uncertainty analysis case	Dwell-time for progressive CIS	Proportion of cancers initiating directly as local invasive cancer	Mammography sensitivity for CIS	References
1	5.22 years	0%	40% for ages over 50 years. 28% for ages less than 50	(14)
2	3 months	0%	88%	(37)
3	5 months	0%	88%	(37)
4	2 years	18.9%	40%	(30)
5	15 years	18.9%	40%	(30)

Table S15: Uncertainty analysis on CIS pathways- Comparing LY saved per 1000 women, and false positives per 1000 women for Peru between basecase and CIS uncertainty cases 1 to 5

Number of lifetime screens	Life years (LY) saved per 1000 women (base case)	Life years saved per 1000 women (case 1)	Life years saved per 1000 women (case 2)	Life years saved per 1000 women (case 3)	Life years saved per 1000 women (case 4)	Life years saved per 1000 women (case 5)	False positives per 1000 women (base case)	False positives per 1000 women (case 1)	False positives per 1000 women (case 2)	False positives per 1000 women (case 3)	False positives per 1000 women (case 4)	False positives per 1000 women (case 5)
1	19	12	6	6	8	12	129	131	114	115	208	136
2	31	20	12	12	14	22	220	221	206	207	295	234
3	44	28	16	17	20	30	315	310	296	295	385	325
4	54	33	21	22	25	36	395	387	368	372	461	420
5	62	38	25	26	30	42	489	480	455	455	546	513
6	70	44	28	29	34	47	579	568	514	518	640	576
7	78	49	32	33	38	52	676	656	589	610	718	661
8	84	53	35	36	42	56	766	741	686	685	790	749
9	88	57	39	40	45	60	842	792	778	778	875	839
10	95	62	42	43	49	63	939	881	860	868	963	925
11	99	66	45	47	52	66	978	970	945	945	1,060	1,011
12	101	69	48	49	56	67	1,055	1,054	1,018	1,018	1,078	1,095
13	105	73	50	51	58	71	1,132	1,129	1,046	1,060	1,166	1,176
14	107	75	52	54	61	72	1,213	1,210	1,133	1,135	1,248	1,259
15	112	78	54	56	63	75	1,302	1,295	1,215	1,216	1,334	1,331

Note: Costs and benefits are undiscounted

Table S16: Uncertainty analysis on CIS pathways- Comparing cost per 1000 women, cost per LY saved saved for Peru between basecase and CIS uncertainty cases 1 to 5

Number of lifetime screens	Cost per 1000 women (basecase)	Cost per LY saved (basecase)	Cost per 1000 women (case 1)	Cost per LY saved (case 1)	Cost per 1000 women (case 2)	Cost per LY saved (case 2)	Cost per 1000 women (case 3)	Cost per LY saved (case 3)	Cost per 1000 women (case 4)	Cost per LY saved (case 4)	Cost per 1000 women (case 5)	Cost per LY saved (case 5)
1	135,788	4,376	135,830	7,149	129,024	12,526	129,062	12,276	138,641	10,466	131,019	7,090
2	192,122	4,499	193,458	6,875	188,063	11,258	188,358	10,865	188,370	9,290	193,832	6,883
3	252,467	4,541	250,243	7,113	246,328	11,826	244,601	11,196	244,033	9,409	252,667	6,981
4	303,885	4,653	299,973	7,474	292,776	11,213	293,991	10,909	301,988	9,765	314,130	7,401
5	363,927	5,021	360,229	7,993	348,899	11,562	347,972	11,262	351,312	9,847	373,950	7,776
6	421,727	5,273	416,699	8,362	387,080	11,733	388,623	11,418	405,595	10,300	415,552	7,827
7	484,359	5,535	473,416	8,600	435,981	11,965	447,694	11,918	466,612	10,710	471,040	8,240
8	542,360	5,830	528,402	8,979	498,311	12,581	496,824	12,212	516,815	10,883	527,786	8,664
9	591,269	6,121	561,846	8,901	557,611	12,762	556,120	12,382	563,390	11,248	586,271	9,097
10	654,089	6,331	619,480	9,129	610,658	13,050	614,314	12,903	618,502	11,516	642,001	9,530
11	680,196	6,339	676,791	9,470	665,225	13,397	664,028	13,055	674,917	11,878	697,797	9,962
12	730,554	6,712	731,399	9,782	713,079	13,762	711,823	13,407	737,388	12,281	752,753	10,528
13	780,415	6,931	780,252	9,980	731,854	13,564	740,038	13,306	750,856	12,054	805,382	10,788
14	832,693	7,290	832,282	10,359	788,329	14,006	788,392	13,516	807,695	12,398	859,501	11,259
15	890,442	7,480	887,648	10,725	841,214	14,406	840,664	14,011	860,801	12,817	906,150	11,459

Note: Costs and benefits are undiscounted

Table S17: Uncertainty analysis on CIS pathways- Comparing QALYs saved per 1000 women and cost per QALY saved for Peru between basecase and CIS uncertainty cases 1 to 5

Number of lifetime screens	QALY saved per 1000 women (base case)	QALY saved per 1000 women (case 1)	QALY saved per 1000 women (case 2)	QALY saved per 1000 women (case 3)	QALY saved per 1000 women (case 4)	QALY saved per 1000 women (case 5)	Cost per QALY saved (basecase)	Cost per QALY saved (case 1)	Cost per QALY saved (case 2)	Cost per QALY saved (case 3)	Cost per QALY saved (case 4)	Cost per QALY saved (case 5)
1	22	13	7	7	9	14	3,825	6,184	10,125	10,044	10,466	6,301
2	37	24	14	14	17	24	3,805	5,928	9,558	9,342	9,290	6,206
3	51	32	19	20	24	33	3,940	6,105	10,176	9,582	9,409	6,256
4	62	39	25	26	29	40	4,056	6,352	9,431	9,264	9,765	6,638
5	72	45	30	31	35	47	4,334	6,857	9,757	9,505	9,847	7,010
6	80	51	34	35	40	52	4,593	7,173	9,694	9,519	10,300	7,080
7	89	57	38	39	45	57	4,877	7,398	9,899	10,018	10,710	7,448
8	95	61	42	43	49	61	5,158	7,752	10,562	10,258	10,883	7,851
9	101	66	46	48	53	65	5,342	7,697	10,836	10,521	11,248	8,283
10	107	71	50	51	57	68	5,609	7,954	11,051	10,993	11,516	8,675
11	112	75	54	55	61	71	5,627	8,292	11,384	11,110	11,878	9,069
12	115	79	56	58	64	73	5,896	8,582	11,686	11,407	12,281	9,561
13	119	83	59	60	67	77	6,099	8,758	11,479	11,349	12,054	9,833
14	122	86	61	63	70	79	6,412	9,076	11,946	11,551	12,398	10,245
15	129	89	64	66	73	82	6,640	9,405	12,286	11,986	12,817	10,470

Note: Costs and benefits are undiscounted

Table S18: Uncertainty analysis on CIS pathways- Comparing number of lifetime screens under different scenarios for both Peru and the US

Number of lifetime screens	Basecase		Case 1		Case 2		Case 3		Case 4		Case 5	
	Peru	US	Peru	US	Peru	US	Peru	US	Peru	US	Peru	US
1	51-51	_	52-52	_	61-61	_	60-60	_	53-53	_	47-47	_
2	50-56	_	50-55	_	53-62	61-66	52-61	_	52-60	_	44-48	_
3	46-57	_	50-57	_	50-63	60-70	51-63	61-70	52-62	60-71	44-51	_
4	45-60	_	50-60	_	52-65	57-71	51-64	57-71	50-63	56-71	44-52	_
5	44-61	_	46-61	_	51-66	55-71	51-66	54-71	50-64	56-72	43-53	_
6	44-62	_	46-62	_	52-70	53-72	51-70	54-72	50-66	53-72	42-54	_
7	41-62	_	46-63	50-68	51-71	53-72	48-70	52-72	47-66	52-73	42-55	_
8	40-63	_	45-63	50-69	46-71	52-73	47-71	52-73	46-67	51-73	41-56	45-61
9	42-64	_	45-64	46-69	45-71	51-73	46-71	51-73	46-70	51-73	40-56	43-61
10	41-64	47-68	44-64	45-70	47-72	51-74	45-72	48-74	45-70	50-73	40-57	41-61
11	40-64	45-68	43-64	46-70	45-72	49-74	45-72	47-74	44-70	48-74	40-58	42-62
12	41-66	44-68	41-65	43-70	44-73	50-75	44-73	47-74	42-71	48-74	41-59	42-62
13	40-66	43-68	42-65	44-70	44-73	46-75	44-73	47-75	44-71	47-75	40-60	41-62
14	41-67	41-68	42-66	43-70	42-74	45-75	43-73	46-75	42-72	46-75	41-61	41-62
15	40-67	41-69	42-66	44-71	42-74	45-76	42-74	45-76	41-72		38-61	40-62

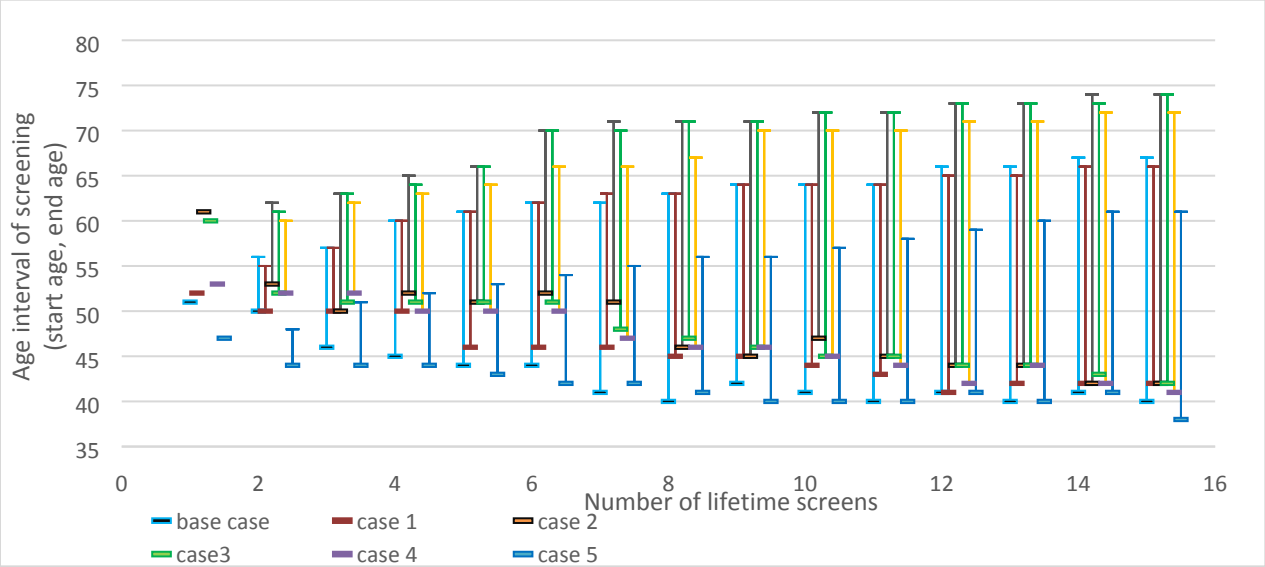

Figure S8: Uncertainty analysis on CIS pathways- Comparing screening age intervals for Peru between basecase and CIS uncertainty analysis cases 1 to 5

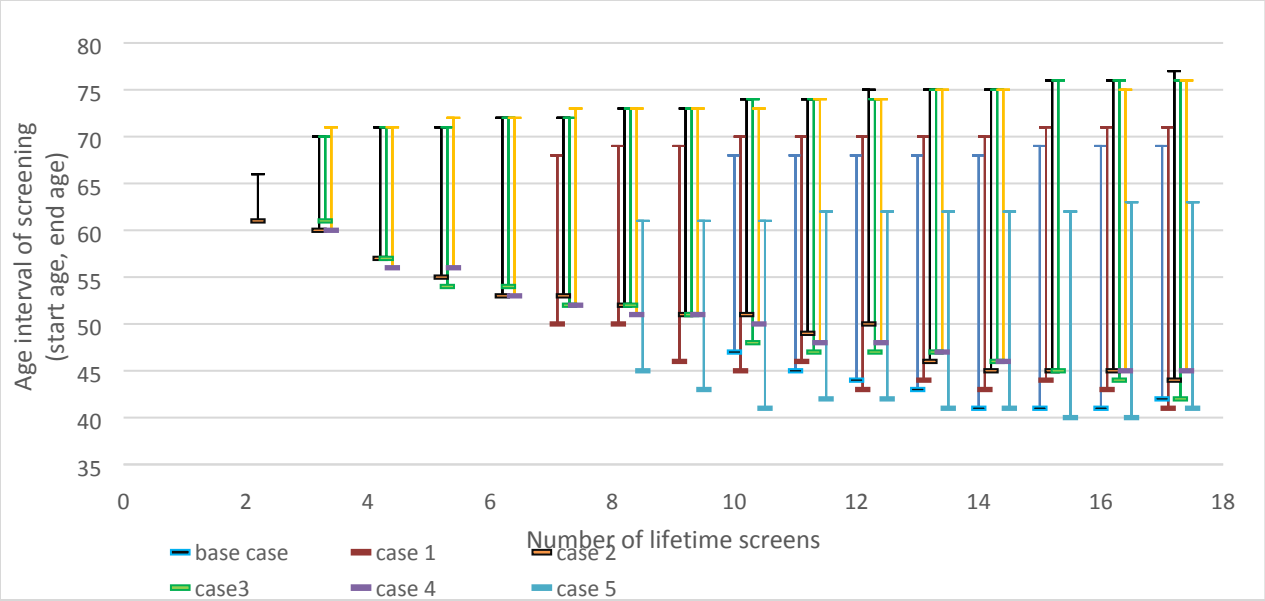

Figure S9: Uncertainty analysis on CIS pathways- Comparing screening age intervals for the US between basecase and CIS uncertainty analysis cases 1 to 5

References

1. Mandelblatt J, Schechter C, Lawrence W, Yi B, Cullen J. Chapter 8: The spectrum population model of the impact of screening and treatment on US breast cancer trends from 1975 to 2000: Principles and practice of the model methods. JNCI Monographs. 2006 Oct 1; 36: p. 47-55.

2. Tan SY, Oortmarssen GJv, Koning HJd, Boer R, Habbema JDF. The MISCAN-Fadia Continuous Tumor Growth Model for Breast Cancer. 2006; 36.

3. Tan K, Simonella L, Wee H, Roellin A, Lim Y, Lim W, et al. Quantifying the natural history of breast cancer. British journal of cancer. 2013 Oct; 109(8): p. 2035.

4. Fryback D, Stout N, Rosenberg M, Trentham-Dietz A, Kuruchittham V, Remington P. Chapter 7: The Wisconsin breast cancer epidemiology simulation model. JNCI Monographs. 2006 Oct 1; 36: p. 37-47.

5. Duffy S, Day N, Tabár L, Chen H, Smith T. Markov models of breast tumor progression: some age-specific results. JNCI Monographs. 1997 Jan 1; 22: p. 93-7.

6. Tabar , Vitak , Chen , Prevost , Duffy. Update of the Swedish Two-County Trial of breast cancer screening: histologic grade-specific and age-specific results. Swiss surgery. 1999 Oct 1; 5(5): p. 199-204.

7. Ferlay J, Soerjomataram I, Ervik M, Dikshit R, Eser S, Mathers C, et al. GLOBOCAN 2012: estimated cancer incidence, mortality and prevalence worldwide in 2012. Int J Cancer. 2012; 136:E359-86.

8. Torre L, Bray F, Siegel R, Ferlay J, Lortet-Tieulent J, Jemal A. Global cancer statistics, 2012. CA Cancer J Clin. 2015 March 01; 65(2): p. 87-108.

9. Gopalappa C, Guo J, Meckoni P, Munkhbat B, Pretorius C, Lauer J, et al. A Two-Step Markov Processes Approach for Parameterization of Cancer State-Transition Models for Low-and Middle-Income Countries. Medical Decision Making. 2018; 38(4): p. 520-530.

10. World Health Organization. Tackling NCDs: 'best buys' and other recommended interventions for the prevention and control of noncommunicable diseases. [Online].: WHO; 2017 [cited 2019 March 18. Available from: https://apps.who.int/iris/handle/10665/259232.

11. World Health organization. CANCER INTERVENTIONS TECHNICAL BRIEFING. [Online].: WHO; 2017 [cited 2019 March 18. Available from: https://www.who.int/ncds/governance/Cancers-FINAL-18May.pdf?ua=1.

12. Ralaidovy AH, Gopalappa C, Ilbawi A, Pretorius C, Lauer JA. Cost-effective interventions for breast cancer, cervical cancer, and colorectal cancer: new results from WHO-CHOICE. Cost Effectiveness and Resource Allocation. 2018; 16(1): p. 38.

13. IARC WHO. GLOBOCAN 2012: Estimated Cancer Incidence, Mortality and Prevalence Worldwide. [Online].; 2012 [cited 2018 February 12. Available from: http://globocan.iarc.fr/Pages/age-specific_table_sel.aspx.

14. Okonkwo QL, Draisma G, der Kinderen A, Brown ML, de Koning HJ. Breast cancer screening policies in developing countries: a cost-effectiveness analysis for India. Journal of the National Cancer Institute. 2008; 100(18): p. 1290-1300.

15. Groot MT, Baltussen R, Uyl-de Groot CA, Anderson BO, Hortobágyi GN. Costs and health effects of breast cancer interventions in epidemiologically different regions of Africa, North America, and Asia. The Breast Journal. 2006; 12(s1).

16. Zelle SG, Baltussen R, Otten JD, Heijnsdijk EA, van Schoor G, Broeders MJ. Predicting the stage shift as a result of breast cancer screening in low-and middle-income countries: a proof of concept. J Med Screen. 2015 March 01; 22(1): p. 8-19.

17. Torre LA, Bray F, Siegel RL, Ferlay J, Lortet-Tieulent J, Jemal A. Global cancer statistics. CA: a cancer journal for clinicians. 2015 March 01; 65(2): p. 87-108.

18. Cronin KA, Mariotto AB, Clarke LD, Feuer EJ. Additional Common Inputs for Analyzing Impact of Adjuvant Therapy and Mammography on U.S. Mortality. Journal of the National Cancer Institute Monographs. 2006.

19. Vallejos CS, Gómez HL, Cruz WR, Pinto JA, Dyer RR, Velarde R, et al. Breast cancer classification according to immunohistochemistry markers: subtypes and association with clinicopathologic variables in a peruvian hospital database. 2010; 10(4).

20. Zelle SG, Vidaurre T, Abugattas JE, Manrique JE, Sarria G, Jeronimo J, et al. Cost-effectiveness analysis of breast cancer control interventions in Peru. PLoS One. 2013; 8(12), e82575.

21. Rojas TV. INEN Global Perspectives, Natonal Cancer Control Plan: "Plan Esperanza". Lima, Peru:; 2016.

22. Zhang J, Mason JE, Denton BT, Pierskalla WP. Applications of operations research to the prevention, detection, and treatment of disease. Wiley Encyclopedia of Operations Research and Management. Wiley. 2011.

23. Rehani M, Vassileva J. Survey of imaging technology and patient dose recording practice in developing countries. Radiation protection dosimetry. 2018 Feb 9; 181(3): p. 240-5.

24. Stout NK, Lee SJ, Schechter CB, Kerlikowske K, Alagoz O, Berry D, et al. Benefits, harms, and costs for breast cancer screening after US implementation of digital mammography. JNCI: Journal of the National Cancer Institute. 2014; 106(6).

25. International Agency for Research on Cancer. Breast cancer screening Volume 15. Lyon Cedex 08, France:; 2016.

26. World Health Organization. WHO position paper on mammography screening. [Online].; 2014 [cited 2019 March 27. Available from: http://apps.who.int/iris/bitstream/10665/137339/1/9789241507936_eng.pdf?ua=1&ua=1.

27. Yankaskas BC, Haneuse S, Kapp JM, Kerlikowske K, Geller B, Buist DSM. Performance of First Mammography Examination in Women Younger Than 40 Years. Journal of National Cancer Insitute. 2010; 102(10): p. 692-701.

28. BCSC. BREAST CANCER SURVEILLANCE CONSORTIUM. [Online]. [cited 2019 March 4. Available from: http://www.bcsc-research.org/statistics/performance/screening/2008/perf_age_time.html.

29. Lee S, Zelen M. Chapter 11: A Stochastic Model for Predicting the Mortality of Breast Cancer. JNCI Monographs. 2006; 2006(36): p. 79–86.

30. Ryser MD, Worni M, Turner EL, Marks JR, Durrett R, Hwang ES. Outcomes of Active Surveillance for Ductal Carcinoma in Situ: A Computational Risk Analysis. JNCI: Journal of the National Cancer Institute. 2016 May; 108(5): p. djv372.

31. De Gelder R, Heijnsdijk EA, Van Ravesteyn NT, Fracheboud J, Draisma G, De Koning HJ. Interpreting overdiagnosis estimates in population-based mammography screening. Epidemiologic reviews. 2011; 33(1): p. 111-121.

32. Lee SJ, Li X, Huang H, Zelen M. The Dana-Farber CISNET model for breast cancer screening strategies: An update. Medical Decision Making. 2018; 38((1_suppl)): p. 44S-53S.

33. Schechter CB, Near AM, Jayasekera J, Chandler Y, Mandelblatt JS. Structure, function, and applications of the Georgetown–Einstein (GE) breast cancer simulation model. Medical Decision Making. 2018; 38(1_suppl): p. 66S-77S.

34. Draisma G, Fracheboud J. Overdiagnosis and overtreatment of breast cancer: microsimulation modelling estimates based on observed screen and clinical data. Breast cancer research: BCR. 2006; 8(1): p. 202-202.

35. Gunsoy NB, Garcia-Closas M, Moss SM. Modelling the overdiagnosis of breast cancer due to mammography screening in womenaged 40 to 49 in the United Kingdom. Breast cancer research. 2012; 14(6): p. R152.

36. van Ravesteyn NT, Van Den Broek JJ, Li X, Weedon-Fekjær H, Schechter CB, Alagoz O, et al. Medical Decision Making. Modeling ductal carcinoma in situ (DCIS): An overview of CISNET model approaches. 2018; 38(1_suppl): p. 126S-139S.

37. Yen MF, Tabar L, Vitak B, Smith RA, Chen HH, Duffy SW. Quantifying the potential problem of overdiagnosis of ductal carcinoma in situ in breast cancer screening. European journal of cancer. 2003 Aug 1; 39(12): p. 1746-54.